Universidade de Aveiro
2019
Departamento de Ciências Médicas

Ana Rita Arede Pinho

O efeito das nanopartículas de ZnO nas células germinativas masculinas

The effects of ZnO Nanoparticles on male germ cells

Universidade de Aveiro
2019
Departamento de Ciências Médicas

Ana Rita Arede Pinho

O efeito das nanopartículas de ZnO nas células germinativas masculinas

The effects of ZnO Nanoparticles on male germ cells

dissertação apresentada à Universidade de Aveiro para cumprimento dos requisitos necessários à obtenção do grau de Mestre em Biomedicina Molecular, realizada sob a orientação científica da Professora Doutora Maria de Lourdes Gomes Pereira, Professora associada com agregação do Departamento de Ciências Médicas da Universidade de Aveiro, e sob a coorientação científica da Professora Doutora Sandra Maria Tavares da Costa Rebelo, Professora auxiliar convidada do Departamento de Ciências Médicas da Universidade de Aveiro.

Este trabalho foi financiado pelo iBiMED (Instituto de Biomedicine) - UID/BIM/04501/2013 - UID/BIM/04501/2019 e pelo programa integrado de SR&TD “pAGE – Protein aggregation Across the Lifespan” (referência CENTRO-01-0145-FEDER-000003), cofinanciado pelo programa Centro 2020, Portugal 2020, União Europeia, através do Fundo Europeu de Desenvolvimento Regional; e pelo CICECO-Instituto de Materiais de Aveiro, FCT Ref. UID/CTM/50011/2019, financiados por fundos nacionais através da FCT / MCTES.

Dedico este trabalho aos meus pais, irmã, avós e namorado pelo apoio incansável e por todo o carinho.

o júri

presidente

Dr.ª Ana Gabriela da Silva Cavaleiro Henriques
equiparada a investigadora auxiliar do Departamento de Ciências Médicas da Universidade de Aveiro

Prof.ª Dr.ª Maria Paula Polónia Gonçalves
professora associada do Departamento de Biologia da Universidade de Aveiro

Prof.ª Dr.ª Sandra Maria Tavares da Costa Rebelo
professora auxiliar convidada do Departamento de Ciências Médicas da Universidade de Aveiro

Agradecimentos

Agradeço às minhas orientadoras Professora Doutora Maria de Lourdes Pereira e Professora Doutora Sandra Rebelo pelo carinho com que me receberam, pela disponibilidade e por todos os ensinamentos que me transmitiram, e que levo no meu coração.

A todo o grupo do Laboratório de Neurociências e Sinalização que de uma forma ou de outra me apoiaram, em especial ao André Nadais, à Filipa Martins e à Cátia Pereira pela paciência e amizade com que me ensinaram, ajudaram e responderam às minhas dúvidas. Um sentido obrigada.

A toda a equipa do iBiMED – Institudo de Biomedicina da Universidade de Aveiro pelo apoio ao meu trabalho e por me terem recebido tão bem. Em especial agradeço à Professora Doutora Catarina Almeida e à Mariana Alves.

Às Professoras Doutoras Elisabete Costa e Ana Senos do CICECO-Instituto de Materiais de Aveiro agradeço a gentileza de me facultarem as nanopartículas de óxido de zinco, sem dúvida um grande contributo para este trabalho. Ao Professor Doutor José Carlos Almeida pela simpatia e pelo tempo que disponibilizou para me ajudar a perceber o processo de síntese de nanopartículas de óxido de zinco.

Às minhas colegas e amigas do mestrado agradeço o apoio e amizade, em especial a Ana Basílio, Carolina Matos, Daniela Figueira, Inês Amaral, Margarida Vaz e Matilde Figueiredo.

Aos meus pais João Pedro Pinho e Ana Paula Pinho por todos os sonhos que depositaram em mim e a quem devo todas as conquistas da minha vida. À minha irmã Maria Inês Pinho, aos meus avós e à minha restante família por todo o amor e apoio incondicional na minha vida pessoal e académica. De facto, sem eles tudo seria impossível.

Ao meu namorado Tiago Martins pelo companheirismo, carinho e paciência. Sem dúvida o meu braço direito para os bons e maus momentos da vida.

palavras-chave

Espermatogónia; Nanopartículas de ZnO; Citotoxicidade; Morte Celular; DNA damage; Espécies Reativas de Oxigénio; Citoesqueleto; Nucleoesqueleto

resumo

Atualmente, um novo conceito de nanotecnologia, “a nanomedicina” foi desenvolvido. Certas nanopartículas oferecem um conjunto excecional de características que melhoram a qualidade e a eficácia do diagnóstico e dos tratamentos na medicina. Nanopartículas de óxido de zinco (NPs de ZnO) são um tipo de nanopartículas de óxido de metal muito usadas, por exemplo, em sistemas de administração de fármacos, em bioimagem e no tratamento do cancro. Alguns autores têm-se concentrado no estudo da biossegurança das NPs de ZnO, uma vez que o seu tamanho e área de superfície permitema entrada e acumulação no organismo, o que pode induzir efeitos tóxicos. As NPs de ZnO foram identificadas, como indutoras de citotoxicidade dependente da dose e do tempo de exposição no testículo e em algumas células germinativas masculinas como os espermatozóides e os espermatócitos. Desta forma é importante conhecer as consequências da exposição a NPs de ZnO no primeiro estadio celular da espermatogénese, a espermatogónia. Assim, o objetivo deste trabalho é avaliar os efeitos das NPs de ZnO na espermatogónia.

A linha celular GC-1 spg derivada das espermatogónias de testículos de ratinho foi tratada com diferentes concentrações de ZnO NPs, nomeadamente 0, 1, 5, 8, 10 e 20 μg/ml durante 6 horas e 12 horas. O estudo foi dividido em duas etapas. Inicialmente, a citotoxicidade resultante da exposição a NPs de ZnO foi avaliada através de ensaios de viabilidade, deteção intracelular de ROS, análise da progressão da apoptose/necrose e os níveis de dano no DNA. No final, foram avaliados os níveis de proteínas do citoesqueleto (α-tubulina acetilada, β-tubulina, β-actina e F-actina) e da proteína nuclear interna Sun1. De acordo com os resultados, concentrações elevadas de NPs de ZnO têm um efeito tóxico em GC-1: a viabilidade decresce, a produção intracelular de ROS, o dano no DNA e os níveis de apoptose e necrose aumentam. Também ao nível do citoesqueleto e do nucleoesqueleto foram verificadas alterações significativas.

Em suma, as NPs de ZnO induzem efeitos citotóxicos em células GC-1 de modo dependente da dose e do tempo. Curtos períodos de exposição e baixas concentrações de NPs de ZnO não induzem citotoxicidade em espermatogónias.

keywords Spermatogonia, ZnO Nanoparticles; Cytotoxicity; Cell Death; DNA damage; Reactive Oxigen Species, Cytoskeleton; Nucleoskeleton

abstract

Nowadays, a new concept of nanotechnology, “the nanomedicine” has been developed. Certain nanoparticles offer an exceptional set of characteristics that improve the diagnosis and treatment quality and efficacy on medicine. Zinc Oxide Nanoparticles (ZnO NPs) are a type of metal oxide nanoparticles with an extensive use, for example, in drug delivery systems, bioimaging and cancer therapy. Several authors have focused on biosafety studies of ZnO NPs, as their size and surface area favour the entrance and accumulation in organism, which can induce toxic effects. ZnO NPs have been identified, as a dose and time dependent cytotoxic inducer in testis and in some male germ cells, like spermatozoa and spermatocyte. In this way, it is important to understand the consequences of ZnO NPs exposure on the first cell stage of spermatogenesis, the spermatogonia. Thus, the aim of this work was to evaluate the effects of ZnO NPs on spermatogonia.

GC-1 spg cell line derived from spermatogonia of mouse testes was treated with different concentrations of ZnO NPs, namely 0, 1, 5, 8, 10 and 20 µg/ml for 6 hours and 12 hours. The study was divided into two stages. Firstly, cytotoxicity resulting from exposure to ZnO NPs was evaluated through cell viability assays, intracellular ROS detection, progression of apoptosis/necrosis analysis and levels of DNA damage. At the end, cytoskeleton protein levels (acetylated α-tubulin, β-tubulin, β-actin and F-actin) and the nuclear intern protein Sun1 were assessed.

According with results, higher concentrations of ZnO NPs have a toxic effect in GC-1: viability decreased, ROS intracellular levels production, DNA damage and cell death ratio increase. Further, at cytoskeleton and nucleoskeleton level, significant changes were verified.

In conclusion, ZnO NPs induce cytotoxic effects on GC-1 cells in a time and dose-dependent manner. Short time exposure and low concentration of zinc oxide nanoparticles do not induce cytotoxicity on spermatogonia.

List of Contents

List of Figures

List of Tables

List of Abbreviations

3β-HSD	3β-Hydroxysteroid dehydrogenase
17β-HSD	17β-Hydroxysteroid dehydrogenases
AJ	Adherents Junction
APS	Ammonium Persulfate
BBB	Blood Brain Barrier
BCA	Bicinchoninic Acid
BSA	Bovine Serum Albumin
BTB	Blood Testis Barrier
CAT	Catalase
CM	Crystal Morphology
CTCF	Corrected Total Cryosection Fluorescence
DAPI	4',6-diamidino-2-phenylindole
DCF	2,7-dichlorofluorescein
DCFH	2,7-dichlorodihydrofluorescein
DCFH-DA	2,7-dichlorodihydrofluorescein diacetate
DMEM	Dulbecco's Modified Eagle's Medium
DNA	Deoxyribonucleic Acid
ECL	Enhanced Chemiluminescence
FBS	Fetal Bovine Serum
GET	Germinal Epithelium Thickness

GPx	Glutathione Peroxidase
GRD	Glutathione Reductase
GSH	Reduced Glutathione
GSI	Gonadosomatic Index;
GST	Glutathione S-transferase
H2AX	Histone 2A family member
H_2O_2	Hydrogen Peroxide
HS	Hydrodynamic Size
ICC	Immunocytochemistry
Ip	Intraperitoneal
INM	Inner Nuclear Membrane
KASH	Klarsicht, ANC-1, Syne homology
LINC	Linker of Nucleoskeleton and Cytoskeleton
LGB	Lower Gel Buffer
MDA	Malonaldehyde
MMP	Mitochondrial Membrane Potential
NAC	N-acetyl-L-cysteine
NAD	Nicotinamide Adenine Dinucleotide
NE	Nuclear Envelope
NP	Nanoparticle
Nr5A1	Steroidogenic factor 1
ONM	Outer Nuclear Membrane

PBS	Phosphate-buffered saline solution
PFA	Paraformaldehyde
PI	Propidium Iodide
PS	Phosphatidylserine
RNS	Reactive Nitrogen Species
ROS	Reactive Oxygen Species
RPMI	Roswell Park Memorial Institute medium
SA	Surface Area
SDS	Sodium Dodecyl Sulfate
SDS-PAGE	SDS Polyacrylamide Gel Electrophoresis
SE	Seminiferous Epithelium
SOD	Superoxide Dismutase
ST	Seminiferous Tubule
STD	Seminiferous Tubule Diameter
Sun1	Sad1 and UNC84 domain containing 1
TAC	Total Antioxidant Capacity
TBS-T	Tris-buffered saline-Tween
TEMED	N,N,N',N'-tetramethylethylenediamine
TJ	Tight Junction
TOS	Total Oxidant Status
UGB	Upper Gel Buffer
UV	Ultraviolet Light

WB	Western Blot
Zn^{2+}	Zinc ion
ZnO NPs	Zinc Oxide Nanoparticles

Theme framing

This dissertation was conducted in the scope of an interdisciplinary cooperation between CICECO from Material Engineering Department and iBiMED and Department of Medical Sciences of Aveiro University.

This work is based in two articles which organization was adapted to this work:

- The introduction was adapted from a submitted review article “The impact of Zinc Oxide Nanoparticles for Male (In)Fertility”;
- The materials and methods, results, discussion, conclusion and future perspectives were adapted from research article “Short Time Exposure and Low Concentration of Zinc Oxide Nanoparticles Prevents Cytotoxicity of first cell stage of spermatogenesis”, which will be submitted.

Introduction

1. Introduction

1.1. Spermatogenesis, a sexual maturation process

Spermatogenesis is the process of production and development of the spermatozoa from a complex and interdependent population of germ cells that are regulated by different internal and external influences, where the hypothalamic pituitary axis is the principal contributor (Cheng *et al.*, 2010; Griswold, 2016; Holstein, Schulze and Davidoff, 2003). This process involves four distinctive phases: mitosis, meiosis, spermiogenesis, and spermiation that occurs in different sequential and cyclic stages: 14 stages in rats; 12 stages in mouse and 6 stages in human (Cheng *et al.*, 2010).

Spermatogenesis (Figure 1) occurs in the seminiferous epithelium (SE) of seminiferous tubule (ST). The ST is surrounded by the interstitial tissue where Leydig cells are responsible to produce and release testosterone depending on the hypothalamic pituitary axis regulation being an important factor in spermatogenesis progression (Cheng *et al.*, 2010; Payne and Hardy, 2007).

The male germ cells in ST are surrounded by Sertoli cells, forming the SE a highly specialized microenvironment responsible for spermatogenesis support. The SE is segregated into the basal and the apical compartment by the Blood Testis Barrier (BTB), a protective barrier created by adjacent Sertoli cells via co-existing tight junctions (TJ), adherent junctions (AJ), and desmosome-like junctions. Cell junctions at the Sertoli-Sertoli and Sertoli-germ cell interface are crucial to coordinate different events of spermatogenesis by sending signals back-and-forth between Sertoli and germ cells, in order to precisely regulate spermatogenesis, germ cell movement across the epithelium, and germ cell apoptosis (Cheng *et al.*, 2010; Kretser *et al.*, 1998).

Spermatogonia is the primordial cell stage of spermatogenesis after the stem cell. The spermatogonia arises from the association of primordial stem cell with Sertoli cell, forming the gonocyte. Several types of spermatogonia can be distinguished: A type spermatogonia and B type spermatogonia. During the pre-puberty the A type spermatogonia (2n) multiplicate continuously by mitosis, through the puberty the A type spermatogonia beyond multiplying can differentiate in B type spermatogonia (2n). B type

spermatogonia multiply by meiosis originating spermatocytes. As the process of meiosis comprises two divisions, cells before the first division are called primary spermatocytes and before the second division secondary spermatocytes. Primary spermatocytes are diploid (2n) cells, and secondary spermatocytes are haploid (n) cells that do not undergo deoxyribonucleic acid (DNA) replication and rapidly divide into spermatids (n). The spermatid has a lower DNA content than the spermatocyte and mark the beginning of spermiogenesis, typified by the condensation of genetic material to form the nucleus in the spermatid head, the formation of the acrosome above the spermatid head, the elongation of the tail, and the packaging of the mitochondria into the mid-piece. Spermiogenesis ends and spermiation start when mature spermatids are released from the germinal epithelium, at this point, the free cells are called spermatozoa (n). Spermatozoa enter the tubular lumen for their further maturation in the epididymis (Griswold, 2016; Holstein, Schulze and Davidoff, 2003; Kretser *et al.*, 1998) (Figure 1).

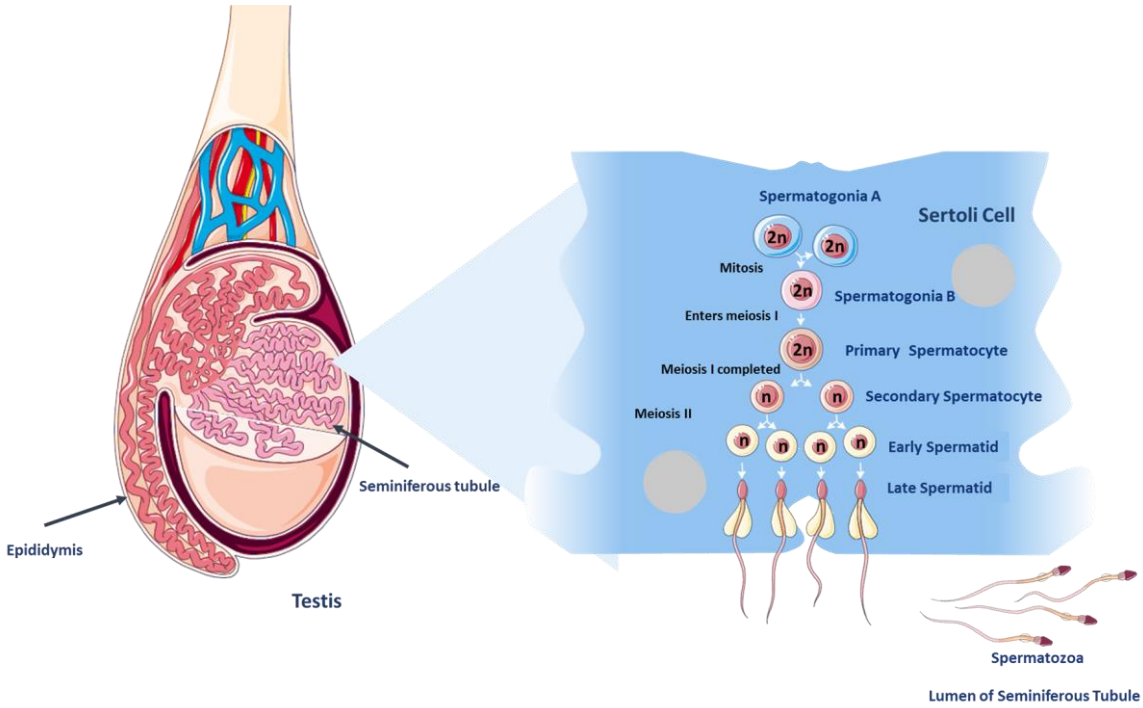

Figure 1: Spermatogenesis process in human testis. (Adapted from: *Sharma and Agarwa, 2011)*

1.2. Nanoparticles and Nanotechnology

Nanoparticles (NPs) are currently defined as particles with less than 100nm length/width in at least one dimension, (Buzea, Pacheco and Robbie, 2007; Dowling *et al.*,

2004; Jeevanandam *et al.*, 2018). At the beginning of the 21st century the interest in nanotechnology have emerged. Nanotechnology was defined as the understand and the control of shape and size matter at the nanometre scale taking into account the future application of NPs (Dowling *et al.*, 2004; Hulla, Sahu and Hayes, 2015; Jeevanandam *et al.*, 2018).

NPs can be classified according the material type, dimension, morphology, composition, uniformity, agglomeration and origin process. Based on the type material used, NPs can be organized into four categories: metallic nanoparticles (e.g. Au, Ag, Cu, Fe, Zn); metal and non-metal oxides (e.g. FeO, VO, AlO, ZnO); semiconductor nanoparticles (e.g. ZnS, CdSe, ZnSe, CdS,) and carbon-based nanoparticles. Regarding origin process, NPs are classified as natural or synthetic. Naturally occurring NPs can be produced by weathering, volcano eruptions, wildfires or microbial processes and include organic and inorganic compounds. Engineered nanomaterials are produced by mechanical grinding, engine exhaust and smoke, or are synthesized by physical, chemical or biological methods. (Buzea, Pacheco and Robbie, 2007; Heiligtag and Niederberger, 2013; Jeevanandam *et al.*, 2018; Król *et al.*, 2017).

NPs have been synthetized in a giant variety of nanostructures. Given that the synthesis methodology determines the latter properties of the material, the choice of preparation method is a very important issue controlling NPs composition, particle size, shape and surface properties (Heiligtag and Niederberger, 2013).

1.3. ZnO NPs characteristics and the importance of synthesis method

Recently, there is growing interest on the metal oxide nanoparticles, like ZnO NPs. Zinc oxide can be called a multifunctional material given its unique physical and chemical properties. Several ZnO NPs applications has been described, from the biomedicine to industry and agriculture.

Before indicating the main properties that made the ZnO NPs an interesting material, is important to note that zinc ion (Zn^{2+}) is the most essential microelement found in all body tissues. Zn^{2+} is located intracellularly, being indispensable for metalloproteins function and provide unique platform for protein subdomains to interact with either DNA

or with other proteins (zinc finger motifs). The biological properties made the ZnO NPs a good alternative to certain others metal nanoparticles, in part by its natural biocompatibility. Besides that, Zn^{2+} is a fairly active element and simultaneously a strong reducing agent that easily oxidize, supporting the formation of ZnO NPs. ZnO NPs has high transparency, low-toxicity, good size, large surface area, good light trapping property, natural abundancy, photoluminescence, good photocatalysis, inexpensive, good semiconductor, high catalytic organic transformation, chemical sensing, bound to several transition metal oxide nanoparticles, stable under UV radiation (Król *et al.*, 2017; Madhumitha, Elango and Roopan, 2016). These extraordinary characteristics made the ZnO NPs an excellent alternative to others metal oxide nanoparticles.

The choice of the preparation method is a very important issue in the design of ZnO NPs depending on the future application. ZnO NPs have been synthetized in a great variety of nanostructures using different chemical, physical and biological methods listed in Figure 2. The variety of methods for ZnO NPs production (Figure 2) makes it possible to obtain nanomaterials with a diversity of sizes, morphological forms and properties, which provide their use in many different applications. Additionally, surface modification methods are also often carried out in order to improve its performance properties according with it future application, complementing the synthesis process (Heiligtag and Niederberger, 2013; Kolodziejczak-Radzimska and Jesionowski, 2014; Król *et al.*, 2017; Madhumitha, Elango and Roopan, 2016).

Figure 2: The variety of physical, chemical and biological methods to synthesize ZnO nanoparticles. (Reproduced from: *Kolodziejczak-Radzimska and Jesionowski, 2014; Król et al., 2017)*

1.4. ZnO Nanoparticles, a variety of applications

1.4.1. Biomedical applications

Nowadays, the variety of ZnO NPs applications have a large spectrum, from agriculture to electronic industry and biomedical applications. The conformational state of ZnO NPs turn this type of nanoparticles very useful. Several are the studies that look for a better conformation to answer the XXI century necessities.

The exceptional properties of ZnO NPs make them an excellent biomedical agent, being able to generate reactive oxygen species (ROS) and to induce apoptosis at higher concentrations (Wang et al., 2015, 2014) and also able to be an antioxidant agent at lower concentrations (Umrani and Paknikar, 2014). These are important characteristics for antimicrobial, anticancer, anti-inflammatory and antidiabetic activities. Additionally, ZnO NPs can be used as a sperm protective agent from cryopreservation and diabetes injuries. Further, ZnO NPs have been successfully exploited as delivery systems for therapeutic agents and also as a bioimage instrument (Jiang, Pi and Cai, 2018; Madhumitha, Elango and Roopan, 2016) (Figure 3).

Although, it is important to note that the effects of ZnO NPs depends of NP size, concentration, morphology, synthesis process and surface area, as well as the type of cell (Nagajyothi *et al.*, 2014; Rad, Sani and Mohseni, 2019; Souza *et al.*, 2019) and organism treated, in the case of bacteria and fungi (Dutta *et al.*, 2012; Król *et al.*, 2017; Lipovsky *et al.*, 2011; Yoshikawa, Possebon and Costa, 2018; Zhang and Xiong, 2015). Small sizes, higher concentrations and high frequency of doses administration potentiates the ZnO NPs effects (Król *et al.*, 2017; Lipovsky *et al.*, 2011; Umrani and Paknikar, 2014; Yoshikawa, Possebon and Costa, 2018).

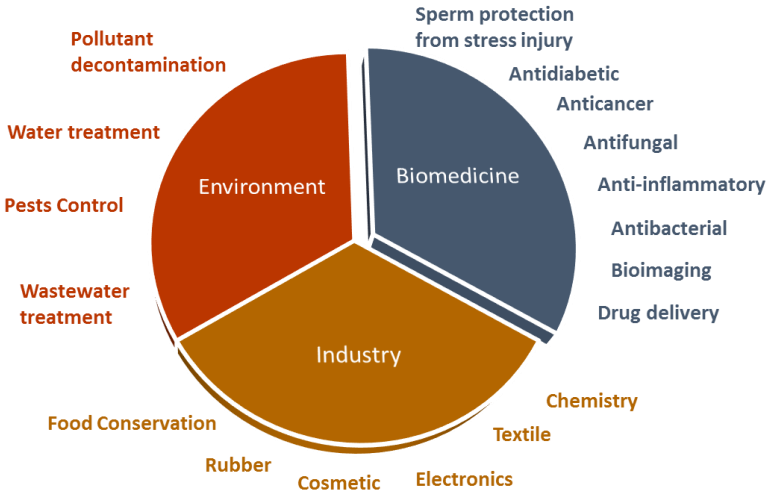

Figure 3: The ZnO nanoparticles, a variety of applications in biomedicine, industry and environment.

1.4.1.1. Antidiabetic activity

ZnO NPs might be used as a promising antidiabetic agent and a diabetes complications reducer (El-Gharbawy, Emara and Abu-Risha, 2016; Jiang, Pi and Cai, 2018). ZnO NPs effectively reverse diabetes-induced pancreatic structural, ultrastructural and functional injury (Umrani and Paknikar, 2014; Wahba *et al.*, 2016), normalize blood glucose (Umrani and Paknikar, 2014; Wahba *et al.*, 2016) and serum insulin levels (El-Gharbawy, Emara and Abu-Risha, 2016; Wahba *et al.*, 2016) and restore the sensitivity of the insulin receptor to insulin (El-Gharbawy, Emara and Abu-Risha, 2016). This is explained because ZnO NPs are an antioxidant agent at lower doses (Umrani and Paknikar, 2014) and zinc acts directly on the insulin signalling pathway (Alkaladi, Abdelazim and Afifi, 2014; Jiang, Pi and Cai, 2018), improving hepatic glycogenesis.

1.4.1.2. Sperm protection from stress injury

Lower doses of ZnO NPs have a protective effect on diabetes rat sperm, due to their antioxidant properties. Sperm from diabetic rats is poor in number and present weak motility. Additionally, the serum testosterone levels are decreased. However, in the presence of ZnO NPs alone or in combination with insulin, an improvement in the quality of sperm and an increase of testosterone production are observed. (Afifi, Almaghrabi and Kadasa, 2015). Furthermore, the use of ZnO NPs in sperm cryopreservation medium has proved to be a protective factor to sperm, preventing common cell damage in cryopreserved sperm, namely DNA damage and cell membrane lipid peroxidation. Moreover, the acrosomal reaction is not altered in cells treated with ZnO NPs relative to control, meaning that this type of nanoparticles does not affect the cell fertility, increasing the motility of sperm compared to cryopreserved sperm (Isaac et al., 2017). However, the sperm underlying protective mechanism is not well known and the majority of studies reported the ZnO NPs as a cytotoxic factor, as will be reviewed in item 1.6.

1.4.1.3. Antibacterial activity

ZnO NPs can be selected as an antibacterial nanomaterial given its differential properties, such as high specific surface area and high capacity to block a wide range of

pathogenic agents (Jiang, Pi and Cai, 2018). ZnO NPs prevent bacteria from adhering, spreading, and breeding in medical devices, very useful in medical applications like pharmaceutical or cosmetic, but also for textile modifications (Jiang, Pi and Cai, 2018; Pasquet *et al.*, 2014).

The main antibacterial toxicity mechanisms of ZnO NPs were based on their ability to increase ROS generation, especially when are exposed to light (Appierot *et al.*, 2009; Jalal *et al.*, 2010; Jiang, Pi and Cai, 2018; Jones *et al.*, 2008; Zhang and Xiong, 2015), causing peroxidation of lipid membrane, leading to its dysfunction and rupture (Dutta *et al.*, 2012; Jalal *et al.*, 2010). Furthermore, the electrostatic interactions of ZnO NPs at high ZnO NPs concentrations with the bacteria surface revealed to be a possible antibacterial mechanism that cause membrane wall damaged (Stoimenov *et al.*, 2002; Zhang *et al.*, 2007). These membrane alterations are a result from transport channels blockages by ZnO NPs that cause starvation and eventually cell death (Dutta *et al.*, 2012). Also, the antibacterial activity may involve the accumulation of ZnO NPs in the outer membrane or in cytoplasm of bacterial cells triggering Zn^{2+} release, and thus bacterial cell membrane disintegration, active transport inhibition, membrane protein damage, and consequent genomic instability and alterations on membrane permeability (Dutta *et al.*, 2012; Heinlaan *et al.*, 2008; Huang *et al.*, 2008; Jiang, Pi and Cai, 2018; Li, Zhu and Lin, 2011).

1.4.1.4. Anti-inflammatory activity

ZnO NPs have different mechanisms for inflammation inhibition very useful in autoimmune (Hanley et al., 2008) and inflammatory diseases and also in drug designing and targeting as well as, in food and cosmetic industry. They may also offer a plausible solution for the treatment of cancer and of various types of inflammation, like from UV rays with minimal side-effects (Agarwal, Nakara e Shanmugam, 2019; Elsayed e Norredin, 2019; Nagajyothi et al., 2015; Wang et al., 2017). Interesting studies regarding atopic dermatitis revealed that ZnO NPs-treatment decrease local skin inflammation of atopic dermatitis on mouse model (Ilves et al., 2014) and of atopic dermatitis patients (Wiegand et al., 2013), as a result from their anti-inflammatory (Ilves et al., 2014; Wiegand et al., 2013), high antioxidative and antibacterial capacity (Wiegand et al., 2013).

1.4.1.5. Antifungal activity

ZnO NPs are also considered as an antifungal agent, making it suitable for food safety and agriculture industries (Król *et al.*, 2017; Lipovsky *et al.*, 2011; Mishra *et al.*, 2017; Sawai and Yoshikawa, 2004). Like in bacterial cells, the increase of ROS production is the main cause of *Candida albicans* cell death and ZnO NPs exposure to blue light enhance the oxidative stress (Lipovsky *et al.*, 2011). Another study have showed that besides ZnO NPs increase the ROS levels, the growth inhibition verified in *Botrytis cinerea* and *Penicillium expansum* is a cause from alterations on fungi morphology in a concentration dependent manner (He *et al.*, 2011). Although, it is important to note that more antifungal studies will be necessary to improve the applications of ZnO NPs as antifungal agent, since, the ZnO NPs effects on yeast organisms studied is still limited.

1.4.1.6. Anticancer activity

ZnO NPs have anticancer properties that are a new alternative to cancer chemotherapy and radiotherapy. They are able to target multiple cancer cell types and simultaneously perform several key functions, including: inhibiting cancer proliferation, drug-resistant cancer sensitization, preventing cancer recurrence and metastasizing, and reactivating cancer immunosurveillance (Wang *et al.*, 2017).

ZnO NPs are a selective anti-cancer agent, inducing higher production of ROS in cancer cells than in normal cells and together with the increased sensitivity of the cancer cells, result in selective cell death of these cells (Król *et al.*, 2017; Ostrovsky *et al.*, 2009). These metal oxide NPs are able to alter the antioxidant mechanisms in cancer cells (Wang *et al.*, 2015), to induce the activation of intracellular apoptosis signalling pathways (Berardis, De *et al.*, 2010) and to cause cell cycle arrest, preventing cell damage passage to the daughter cells. (Setyawati, Tay and Leong, 2013). Moreover, ZnO NPs exhibit a strong preferential ability to kill rapidly dividing cancer cells relative to quiescent cells of the same lineage, suggesting that the mechanisms of ZnO NPs toxicity might be associated with the proliferative potential of the cell. This inherent differential toxicity raises exciting opportunities as anticancer agents, and the selectivity of these

nanomaterials can be expected to be even further enhanced by NP design by linking tumor targeting ligands to tumor-associated proteins, or by using NPs for drug delivery. These observations may provide the basis for developing of new rational strategies to protect against NP toxicity or enhance the destruction of cancer cells (Hanley *et al.*, 2008).

1.4.1.7. Bioimaging

Furthermore, ZnO NPs are considered very useful, safe and cheap for biosensing applications (Xiong, 2013; Xiong *et al.*, 2008). Several studies have focused on the production of ZnO NPs, which are able to emit luminescence, making their available for controlling the drug release by bioimage, and assessing imaging information about the organism. Using specific receptor molecules such as antibodies and aptamers to the surface of luminescent ZnO NPs allows the detection of specific proteins, providing a better diagnosis (Jiang, Pi and Cai, 2018; Zhang and Xiong, 2015). ZnO NPs are able to detect with high selectivity and sensitivity dopamine, a biomarker for schizophrenia, Parkinson, and Alzheimer diseases (Zhao *et al.*, 2013), carbohydrate antigen 19-9, a marker of pancreatic cancer (Gu *et al.*, 2011) and picric acid, a toxic compound that cause anaemia, headache, and liver injury (Singh *et al.*, 2014). Moreover, ZnO NPs allow tracing metastasis and are potentially amenable for multicolour tumour detection (Kang *et al.*, 2017). The fluorescence emissions of ZnO NPs can be detect during live-cell imaging experiments using a confocal microscope, which may help in deciphering their complex interactions with various cells types (Eixenberger *et al.*, 2019) and could be used as effective labelling probes in cell culture in short time (Liu *et al.*, 2011) and *in vivo* studies (Kang *et al.*, 2017; Liu *et al.*, 2011). In future, ZnO NPs can provide a better reliability of the collected data as a dual modal fluorescence and magnetic resonance imaging, once combine the high sensitivity with the spatial resolution, respectively (Liu *et al.*, 2011).

1.4.1.8. Drug Delivery

The use of ZnO NPs as drug delivery system offer some advantages that solve serious limitations of a common drug carrier, such as: enhance the circulation of drugs for considerable periods of time, maintain the relevant therapeutic concentrations and facilitate the adsorption of drug (Tripathy *et al.*, 2015). ZnO NPs application in cancer treatment has been increased, through the loading of anticancer drugs into these nanoparticles. Nanoparticles are small enough to pass through the capillaries, to target specific sites of cancer cells and also allow a controlled release of the drug, reducing the overall amount of drugs used and minimizing undesirable side effects. The anticancer activity of ZnO NPs synergizes the therapeutic activity of drug loaded, contributes to a more effective drug cancer treatment. Furthermore, it provides better targeting of the highly toxic chemotherapeutic drugs, a control release of drug and at the same time, showed low toxicity towards normal cells, producing very few side effects (Jiang, Pi and Cai, 2018; Mishra *et al.*, 2017; Rasmussen *et al.*, 2010; Sharma *et al.*, 2016; Wang *et al.*, 2017). ZnO NPs are also useful for DNA transfer, for real time imaging of gene transfer, for targeted gene delivery and gene silencing and also for next-generation cancer applications (Ghaffari et al., 2017; Rasmussen et al., 2010; Zhang et al., 2013).

1.4.2. Other applications, besides biomedicine

Nowadays, the variety of ZnO NPs applications have a large spectrum, from agriculture to electronic industry (Figure 3). The water, our not infinite vitally natural resource is becoming scarcer, and its availability is the major social and economic concern. ZnO NPs have emerged as another efficient candidate in water and wastewater treatment because of their unique characteristics, such as light absorption limited in the ultraviolet light region, strong oxidation ability, biocompatible and good photocatalytic property that allow the removal of various pollutants from water (Lu *et al.*, 2017). Together with the water treatment are the capacity to photocatalysis, a process capable to decontaminate the environment. The photoluminescence properties of ZnO NPs allows the detection of Co^{2+} and Cu^{2+}, environmental pollutants based on the quenching of their luminescence. Also, the ZnO NPs are capable to promote the photocatalytic degradation

of *Escherichia coli* bacteria in water, which might be employed in the development of passive systems to improve water quality in isolated areas (Rodríguez *et al.*, 2010).

In agriculture, the antimicrobial activity of ZnO NPs is extremely useful, once can help to control pests. The antifungal activity of ZnO NPs against *Botrytis cinerea* and *Penicillium expansum*, a fungus responsible for serious problems in agriculture, turn these nanoparticles an effective fungicide in agricultural and in food safety applications (He *et al.*, 2011). These metal nanoparticles could be also used as a fertilizer. The germination improved, root growth, shoot growth dry weight and pod yield of the ZnO NPs-treated peanut seeds might be explained by the higher concentrations of zinc present in these nanoparticles (Prasad *et al.*, 2012). This type of nanofertilizer plays an important because it not only supplies nutrients for the plant and can be used in very small amounts, but also revives the soil to an organic state (Sabir, Arshad and Chaudhari, 2014).

ZnO NPs are firstly applied in the rubber industry as they can provide wearproof of the rubber composite, improve performance of high polymer in their toughness and intensity and antiaging, and other functions. Besides that, the ZnO NPs are an interesting material for optoelectronic, since they have fluorescent and electrochemical properties (Jiang, Pi and Cai, 2018; Mikrajuddin *et al.*, 2002).

1.5. ZnO Nanoparticles: route of entrance and accumulation in organism

Despite nanotechnology being a contemporary science, the human exposure to nanoparticles has occurred throughout human history and was dramatically increased during the industrial revolution (Hulla, Sahu and Hayes, 2015). Of note, when the industrial emissions did not fulfil the current environmental and public health safety standards, human exposition to NPs is inevitable and uncontrolled. Currently, despite the industrial emissions standard are regulated, the number of NPs applications increased. Furthermore, new NPs commercial applications have been developed, involving new properties, leading to new biological interactions and unexpected toxicity (Walker and Bucher, 2009).

Due to their small size, NPs have the ability to penetrate the skin, the lungs, the gastrointestinal tract and also blood brain barrier (BBB) (Figure 4) (Lan and Yang, 2012).

These tissues, except the BBB are in constant contact with the environment, facilitating NP entrance. Additionally, injections and implants are other possible routes of exposure. Thus, nanoparticles can translocate into the circulatory and lymphatic systems, and ultimately to body tissues and cells, though interaction with subcellular structures (Buzea, Pacheco and Robbie, 2007).

ZnO NPs are a type of nanomaterial with a huge demand in biomedicine, industry, agriculture, among others areas, which implies that the human exposure to ZnO NPs is high, and like the generality of NPs, they can invade the human organism tissues, and their cells. ZnO NPs have been described as an easily accumulating nanomaterial, whose accumulation rate differs between tissue type. Liver, kidney, lung, brain and spleen are the organs with high ZnO NPs accumulation levels (Chen *et al.*, 2016), presenting signals of cytotoxicity as a consequence of that exposure (Figure 4) (Abbasalipourkabir *et al.*, 2015; Hao *et al.*, 2017; Kuang *et al.*, 2016; Lin *et al.*, 2015). Besides that, metal nanoparticles have the capacity to cross the BTB, in part by its size but also by the production of an inflammatory response that compromise the BTB integrity (Lan and Yang, 2012). BTB controls the adluminal environment in which germ cells develop by influencing of its chemical composition, so changes on it is a risk to spermatogenesis (Cheng *et al.*, 2010; Kretser *et al.*, 1998). It is possible to speculate that ZnO NPs may also cross the BTB, inducing testicular toxicity (Figure 4). However, the knowledge on how ZnO NPs cross BTB is indispensable for assessing this toxic mechanism in the male reproductive system.

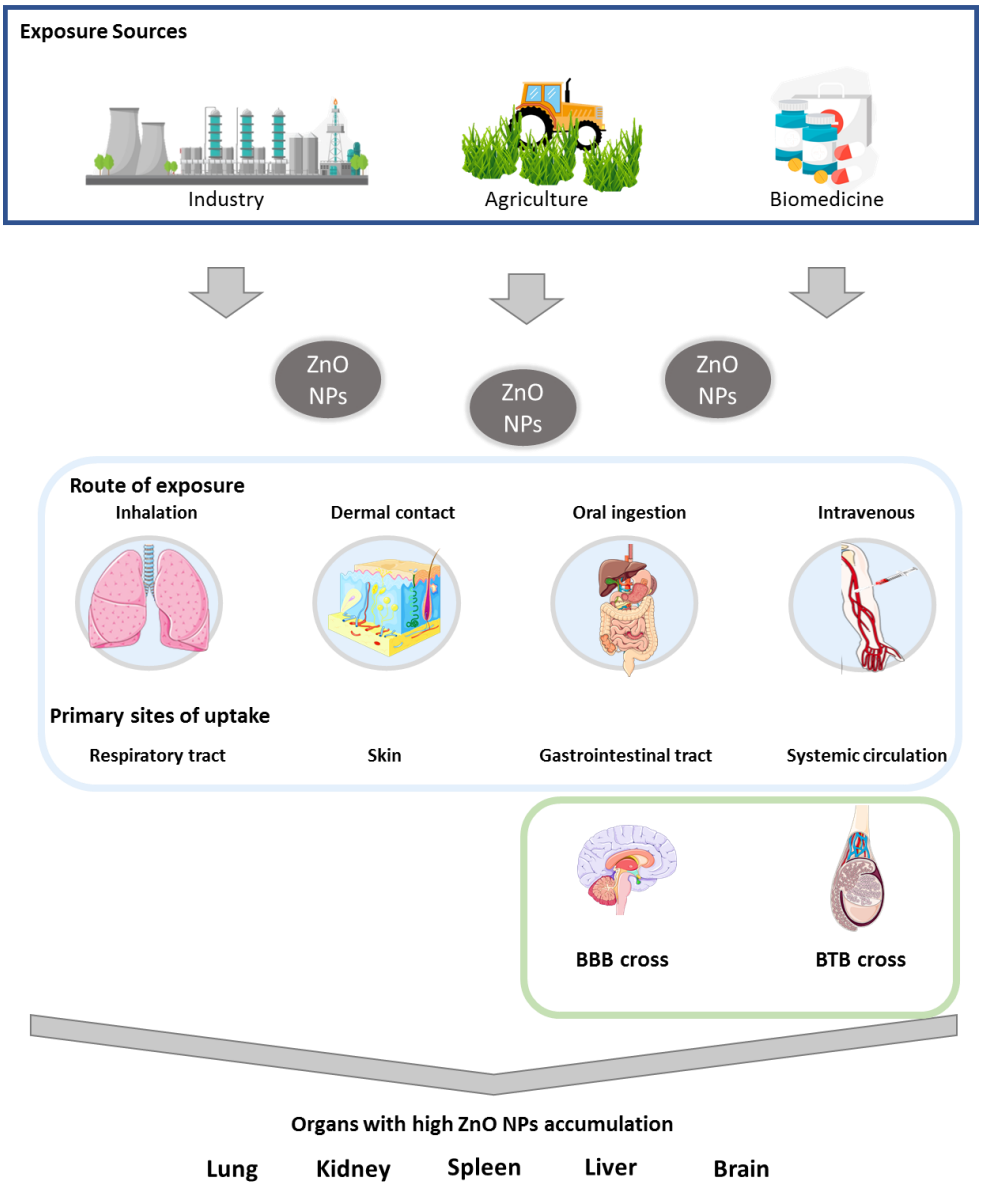

Figure 4: Routes of ZnO NPs invasion an accumulation in human organism BBB- Blood Brain Barrier; BTB- Blood Testis Barrier. (Adapted from: *Ispanixtlahuatl-Meráz, Schins and Chirino, 2018)*.

1.6. ZnO Nanoparticles and is effects on male reproductive system– *in vitro* and *in vivo* studies

As described above, the variety of ZnO NPs applications is wide. Considering that human exposure to this type of metallic nanoparticles is high, it is relevant and essential to evaluate the effects of the ZnO NPs at several levels, including the histological, cellular and molecular levels. Some studies have focused on the effects of ZnO NPs on spermatogenesis and have suggested that ZnO NPs have a detrimental impact on male

reproductive health. Tables 1 and 2 display representative studies, summarizing the main conditions and factors of *in vitro* and *in vivo* studies, respectively.

1.6.1. *In vitro* studies

Only three *in vitro* studies were performed to determine cytotoxic effects of ZnO NPs on male reproductive health (Table 1). The *in vitro* analysis of ZnO NPs effects on spermatogenesis particularly on male germ cells are scarce and they mainly focused on the evaluation of cytotoxicity of different types of cells. From all over the stages of spermatogenesis, the cytotoxicity of ZnO NPs were analysed only at few cell stages, namely spermatocyte and spermatozoa, which indicates that their effect on male germ cells is not well established and deserves further investigation. In addition, the effects on regulatory and supportive cells, the Sertoli cells and Leydig cells, were also analysed and discussed. All the studies were performed on mouse cell lines except one that uses human sperm samples. Viability, ROS production levels, DNA damage and apoptosis levels were the parameters evaluated in these studies (Table 1).

The BTB is a crucial component for normal spermatogenesis function. Previous studies evaluated the expression of tight junction proteins in Sertoli cells, namely claudin-5, occludin, ZO-1, and connexin-43, which promote the adhesion between Sertoli cells forming the BTB (Liu *et al.*, 2016). As a consequence of ZnO NPs exposure an increased ROS production is observed and the expression of these proteins is decreased (Figure 5) (Han *et al.*, 2016; Liu *et al.*, 2016). The authors proposed that ROS possibly activates the Erk1/2 proteins inducing an increase of TNF-α cytokine levels leading to alterations in tight junction proteins (Hellani *et al.*, 2000; Li *et al.*, 2006). Therefore, is possible to deduce that the integrity of BTB is altered in the presence of ZnO NPs, which compromises the essential conditions for spermatogenesis progression (Liu *et al.*, 2016). To date is not known how the ZnO NPs cross the BTB.

Table 1: *In vitro* studies of ZnO NPs effects on male germ cells. Abbreviations: BTB- Blood Testis Barrier; DMEM- Dulbecco's Modified Eagle's Medium; GSH - Reduced Glutathione MDA – Malondialdehyde; RPMI- Roswell Park Memorial Institute medium; ROS- Reactive oxygen species; MMP- Mitochondrial Membrane Potential.

ZnO NPs Characteristics	Objective	Cell Type	ZnO NPs Concentration (µg/ml)	Parameters	Results	Reference
Size: 50 nm **Shape:** amorphous	Evaluate the cytotoxic of ZnO NPs on viability of spermatozoa	Spermatozoa (Human)	10, 100, 500, 1000	-Viability	The toxicity depends on concentration and time of exposure; Higher concentrations and higher exposure periods induce higher toxicity.	Barkhordari *et al.*, 2013
Size: 70 nm **Shape:** spherical **Nature:** crystalline **Dispersion:** polydisperse and agglomerate in quasi-spherical and hexagonal structures **Surface roughness:** high (22.9 nm)	Investigate the toxicity of ZnO NPs in testicular cells	Leydig cell Sertoli cell (Mouse)	0, 5, 10, 15, 20	- Cellular uptake of ZnO NPs -Viability; -MMP and ROS levels; -Apoptosis and DNA Damage;	ZnO NP aggregates in the cytoplasm and in nucleus. The toxicity depends on the concentration (≥10µg / ml), the time (≥6h) of exposure and not of Zn^{2+}release; ROS production increase, with loss of MMP which leads to apoptosis associated with nuclear DNA damage;	Han *et al.*, 2016
Size: 177 nm **Shape:** spheroid or ellipsoid **Zeta Potential:** -27.4 ± 1.0 mV **Purity:** >97%	Explore the effects of ZnO NPs of sublethal doses and their underlying mechanisms on male germ cells	Sertoli cell Spermatocyte (Mouse)	0, 0.04, 0.08, 0.4, 0.8, 4, 8 and 16	-Viability -ROS, GSH and MDA levels; -Permeability, MMP and cytochrome C - BTB junction proteins levels; -Erk1/2 and TNF-α levels; -DNA damage and cell cycle;	The sublethal dose of ZnO NP is 8 µg/ml; GSH decrease and MDA increase; Sertoli cell membrane disruption and cellular invasion; ROS production increase which compromises BTB, by down-regulating the expression of BTB proteins, cause DNA damage and arrest S-phase in spermatocyte cell.	Liu *et al.*, 2016

Another interesting study defined the 1000 µg/ml of ZnO NPs concentration as the cytotoxic dose for human sperm cells, given that a significant reduction in cell viability was observed. Additionally, the increase of cell mortality was observed 180 minutes after NPs exposure (Barkhordari *et al.*, 2013). In mouse cells, sublethal dose and time varies between cell type. According with the results in Table 1 the cytotoxicity of ZnO NPs on male reproductive system depends on concentration, time of exposure and also of cell type (Barkhordari *et al.*, 2013; Han *et al.*, 2016; Liu *et al.*, 2016). However, structural characteristics of ZnO NPs for example size and surface area was not considered as a variable of analysis.

The cytotoxic effects of ZnO NPs were also evaluated using mouse spermatocytes (Liu et al., 2016). The authors described an increase in DNA damage and cell cycle alterations, with an increase in cell cycle proteins expression and increase in the number of cells in S-phase with a decrease in G1 and G2 phase (Figure 5). These changes have been reduced by the use of an antioxidant, indicating that oxidative stress plays a role in ZnO NPs cell cycle arrest (Liu *et al.*, 2016).

From all *in vitro* studies analysed, only one studied apoptosis in Leydig and Sertoli cells after exposure to ZnO NPs. These authors found that the apoptosis is associated with ROS formation, with loss of mitochondrial membrane potential, which leads to the increase of apoptosis in Sertoli and Leydig cells associated with nuclear DNA damage (Figure 5) (Han *et al.*, 2016). These results clearly indicate a possible negative effect of ZnO NPs on spermatogenesis progression, since the number of Sertoli and Leydig apoptotic cells increases after exposure to these nanoparticles.

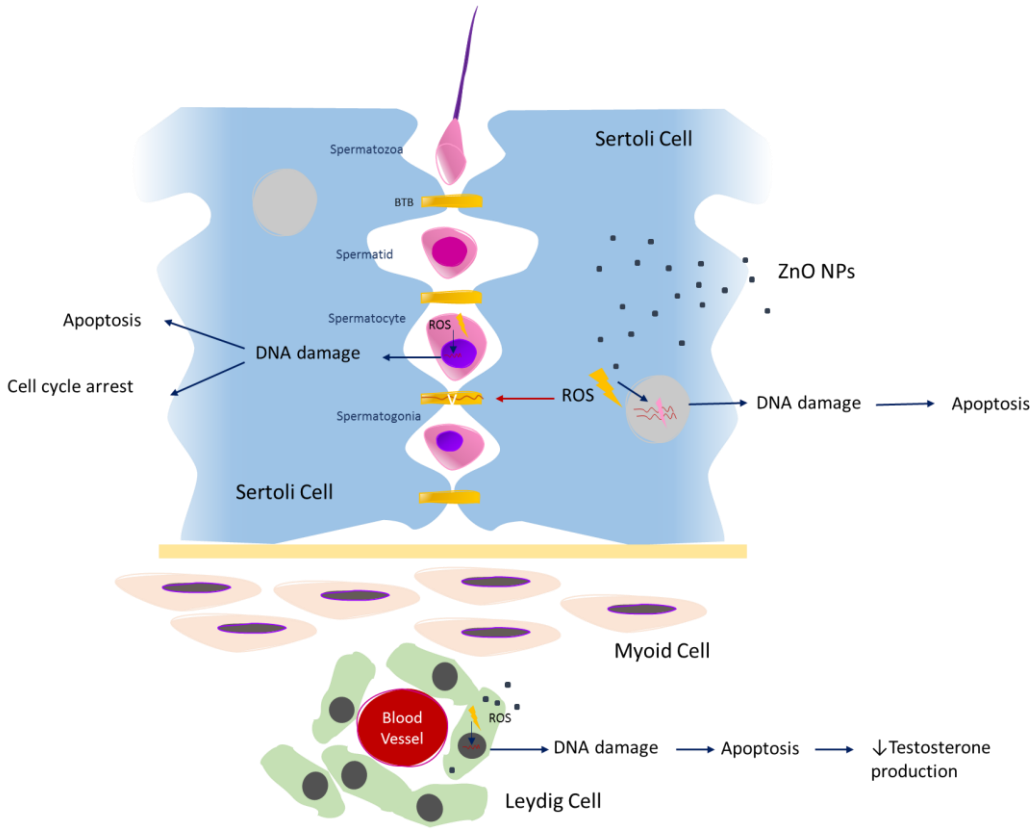

Figure 5: The effects of ZnO NPs on spermatogenesis. BTB- Blood Testis Barrier; ROS- Reactive oxygen species; DNA- Deoxyribonucleic acid; ZnO NPs-Zinc Oxide Nanoparticles.

1.6.2. *In vivo* studies

Several animal models and routes of administration were used to study the *in vivo* consequences of ZnO NPs exposure on spermatogenesis. These *in vivo* studies evaluated the impact of ZnO NPs on male reproductive health using different animal models (Table 2). This type of investigation was important to evaluate the histological and biochemical alterations in testis when exposed to ZnO NPs. Different types of tissues were evaluated and directly related to spermatogenesis.

Most of these studies used rodents to analyse changes using several techniques, including histological and biochemical analysis. In general, the parameters studied included testicular histology, ST diameter and epithelium height, oxidative stress, apoptosis and genotoxicity indicators. Most studies characterized ZnO NPs, although in some studies these data were not available.

Table 2: *In vivo* studies of ZnO NPs effects on male reproductive system and on male fertility. Abbreviations: CAT – Catalase; CM- Crystal Morphology; HS - Hydrodynamic Size; MDA – Malondialdehyde; SOD – Superoxide Dismutase; GPx – Glutathione Peroxidase; GRD - Glutathione Reductase; GSH - Reduced Glutathione; GST - Glutathione S-transferase; TAC - Total Antioxidant Capacity; GSI- Gonadosomatic Index; Ip- Intraperitoneal; SA- Surface Area; SE- Seminiferous Epithelium STD- Seminiferous Tubule Diameter; GET- Germinal Epithelium Thickness.

ZnO NPs Characteristics	Objective	Animal model/ Tissue or organ of study	Administration via of exposure	Evaluated Parameters	ZnO NPs Concentration	Results	Reference
	Evaluate the effects of ZnO NPs on spermatogenesis	NMRI mouse Semen Testis	Oral	-Epididymal sperm -Testicular histology -SE Morphometry	0, 5, 50 and 300 mg/kg	Cytotoxicity in testicular germ cells in a dose dependent manner (≥50 mg/kg): testis histological alterations; abnormal sperm increase; sperm and Leydig cells number reduction.	Talebi, Khorsandi and Moridian, 2013
Size: 10-30 nm; **SA:** 20/30 m^2/g; **Colour:** Milky white; **Crystal phase:** single; **CM:** Nearly spherical; **Density:** 5,606 g/cm^3 **Purity:** ≥99%	Investigate the effects of ZnO NPs on adult male Wistar rats	Wistar rats Epididymis Sperm Blood	Ip	- Epididymal Sperm -Serum Biochemistry: SOD; GPx; MDA; TOS; TAC	0, 50, 100, 150 and 200 mg/kg	Viability and sperm number decrease (≥50 mg/kg); Poor sperm quality (≥100 mg/kg); Antioxidant capacity decrease (200 mg/kg).	Abbasalipour kabir *et al.*, 2015
Size: 20nm **SA: >** 90 m^2/g **Colour:** White **CM:** Nearly spherical **Purity**: ≥99 %	Investigate the effects of ZnO NPs at different doses on testis of adult mice	NMRI male mouse Testis	Ip	-Testicular histology	0, 250, 500 and 700 mg/kg daily	Testis histological alterations; Reduction and degeneration of spermatogonia, primary spermatocyte, spermatid, sperm and Leydig cells; Spermatogenesis arrest;	Mozaffari *et al.*, 2015
Size: 70 nm **Shape:** spherical **Nature:** crystalline **Dispersion:** polydisperse **Surface roughness:** high (22.9 nm)	Investigate the toxicity of ZnO NPs in testicular cells	Cd1 Mouse (21 day old) Epididymis Sperm Testis	Intravenous	-Sperm Morphology -SE Morphometry	0, 1, 5 mg/kg	Spermatogenesis damage by alteration of SE and by inducing sperm abnormalities (≥5mg / kg, ≥49 days).	Han et al., 2016
Size: <50 nm; **SA:** >10.8 m^2/g; **Purity:** >97%;	Evaluate the toxicological effect of ZnO NPs on male fertility and the amelioration with querectin in Wistar Han rats.	Wistar Han rats Epididymis Sperm Testis	Intragastric intubation	-Testis Biochemistry: MDA; CAT; SOD; GPx; GSH; -Epididymal Sperm -Testicular histology; -Serum Testosterone level; 3β-HSD; 17β-HSD; Nr5A1 mRNA expression levels	0, 100, 400 mg/kg	Decrease of sperm live cell and Leydig cell number; Serum testosterone level decrease and increase of abnormal sperm; Atrophy, and necrosis of ST in a dose dependent way; Antioxidant capacity decrease and oxidative stress increase;	Hussein *et al.*, 2016

ZnO NPs Characteristics	Objective	Animal model/ Tissue or organ of study	Administration via of exposure	Evaluated Parameters	ZnO NPs Concentration	Results	Reference
Size: 17,9±7,3 nm **Distribution range:** 1-55nm **HS:** 721±109,5nm **Purity:** ≈100% **Surface area:** 15–25 $g/m^{2;}$	Investigate the effects of ZnO NPs exposure on C. elegans germ cell apoptosis and related gene expressions and compare the apoptosis-inducing effects of ZnO NPs with $ZnCl_2$	*Caenorhabditis elegans* Egg	Mix of ZnO NPs or $ZnCl_2$ into nematode growth medium (NGM) agar	-Apoptosis genes expression: ced-13, ced-3, ced-4, ced-9, cep-1, dpl-1, efl-1, efl-2, egl-1, egl-38, lin-35, pax-2, and sir-2.1.	0, 6.14 $X10^{-1}$, 61.4, and 614 µM	Apoptosis in germ cells (≥61,4 µM) by upregulate apoptosis genes (cep-1, cep-13, efl-2, egl-1, lin-35, and sir-2.1 (≥614µM). Enhanced apoptosis effects were not fully attributed to ionic Zn, ZnO NPs also have the capacity to affect apoptotic machinery.	O'Donnell *et al.*, 2017
Size: 80nm	Investigate side effects of various doses of ZnO NPs on reproductive system of albino mice	Adult Albino mice Testis Prostate Seminal vesicles Epididymis	Oral	-Male reproductive system histology	0, 150, 350 mg/kg	Cytotoxic on testicular tissue in a dose dependent manner; Damages in all tissues of reproductive system (testis, seminal vesicles, prostate and epididymis (350 mg/kg.bw).	Salman, 2017
Size: 39.45 +19.88nm **HS:** 447,5nm **Shape:** hexagonal **Aggregation:** large and irregular **Polydispersity index:** 0,13nm **Zeta Potential:** -32,1mV	Evaluate the genotoxic effect of ZnO NPs in Swiss mice	Swiss male mouse Semen Liver Bone Marrow	Oral	-Semen -Genotoxicity in blood samples: CA; MnPCEs; DNA damage -ROS level in liver	300 – 2000 mg/kg	Genotoxic in a dose-dependent manner by ROS generation of ROS that cause changes (2000 mg/kg): in genomic integrity and anomalies in spermatogenesis; chromosomal alterations and generation of micronucleus in bone marrow cells of male mice.	Srivastav *et al.*, 2017
Size: 10-30 nm	Investigate the effect of ZnONPs on some of the antioxidant parameters of semen plasma, quantitative and qualitative properties of Arabic ram sperm	Arabic sheep Semen	Oral	-Semen -Membrane integrity -SOD and TAC	0, 40, 80 mg/kg	Improves the qualitative and quantitative properties of sperm and some antioxidant parameters of seminal plasma, neutralizing the effects of ROS (80 mg/kg).	Abaspour Aporvari *et al.*, 2018
Size: 10-30nm **Purity:** 99,9%	Investigate the effects of different zinc source (nano, organic and inorganic) supplementations on reproduction of male Japanese quail.	Japanese quail chick (one-day old) Testis Eggs	Oral	-Index of cloacal gland size; -GSI; STD; GET; -Serum testosterone level -Fertility -Hatchability	0, 25, 50 mg/kg	Detrimental effects on reproduction, by reducing hatchability and, also, inducing abnormalities in Japanese quail embryos.	Khoobbakht *et al.*, 2018

1.6.2.1. *In vivo* studies in mammalian animal models

Most *in vivo* studies reported in Table 2 evaluate changes in testicular and epididymal tissue after exposure of rats or mice to different concentrations of ZnO NPs. The histological pattern was similar in both rats or mice, with formation of multinucleated giant cells (Mozaffari *et al.*, 2015; Talebi, Khorsandi and Moridian, 2013), disorganization of germ cells layers, detachment and sloughing of immature germ cells and vacuolization of the epithelium of ST after exposure to a high concentrations of ZnO NPs (Hussein *et al.*, 2016; Mozaffari *et al.*, 2015; Salman, 2017; Talebi, Khorsandi and Moridian, 2013). This histological alteration is indicative of functional damage in Sertoli cells, which is responsible for support and protection of germ cells during spermatogenesis (Talebi, Khorsandi and Moridian, 2013).

Spermatogenesis arrest has been described as a consequence of high concentrations ZnO NPs exposure (Hussein *et al.*, 2016; Mozaffari *et al.*, 2015; Salman, 2017; Talebi, Khorsandi and Moridian, 2013). The appearance of immature germinal cells in the epididymis (Mozaffari *et al.*, 2015), degenerated and desquamated spermatocytes (Hussein *et al.*, 2016; Mozaffari *et al.*, 2015) and sperm cells (Mozaffari *et al.*, 2015) in the lumen of STs and of epididymis, respectively is evident. In addition, the number of germinative cells is reduced (Mozaffari *et al.*, 2015; Talebi, Khorsandi and Moridian, 2013 Hussein *et al.*, 2016) and the STs (Wistar Han rats) were almost empty of spermatid and spermatozoa after exposure to 400 mg/kg of ZnO NPs. The number of Leydig cells, an important cell responsible for testosterone production, also decreased in exposed animals (Ewing and Zirkin, 1983; Payne and Hardy, 2007). These results are consistent with data obtained from *in vitro* study using a Leydig cell line, that report a decrease in Leydig cells viability and an increase of apoptosis after *in vitro* exposure to ZnO NPs (Han et al., 2016) (Figure 5).

Additionally, analysing the morphology of seminiferous tubules, it is notable a decrease in diameter and height of the epithelium resulting from germ cell loss, due to apoptotic effect of ZnO NPs on spermatogenic cells (Han *et al.*, 2016; Khoobbakht *et al.*, 2018; Mozaffari *et al.*, 2015; Talebi, Khorsandi and Moridian, 2013). In addition to the testis and epididymis, other studies analysed histological changes in seminal vesicles and

prostate (Salman, 2017). The occurrence of inflammation in the dilated area of prostate acini and the hyperplasia of epithelial lining cells of prostatic acini was detected in mice exposed to ZnO NPs. In seminal vesicles, the changes were also significant, with the detection of mononuclear cells infiltrating the stroma and the appearance of mild to moderate proliferation of epithelial cells (Salman, 2017). According to these data, exposure to ZnO NPs has repercussions on all male reproductive system in a dose-dependent manner.

Regarding the sperm quantity and quality, ZnO NPs cause harmful effects reducing the number and motility of sperm cells and increasing the number of morphological abnormalities such as double head, small head, formless head, and double tail (Abbasalipourkabir *et al.*, 2015; Han *et al.*, 2016; Hussein *et al.*, 2016; Srivastav *et al.*, 2017; Talebi, Khorsandi and Moridian, 2013). A significant reduction in sperm viability has also been observed in several studies (Abbasalipourkabir *et al.*, 2015; Hussein *et al.*, 2016; Srivastav *et al.*, 2017). Interestingly, Hussein *et al.*, 2016 revealed that these changes in sperm quality could be alleviated by co-exposure of quercetin, a potent anti-oxidant. The number of Leydig cells also decrease after exposure to low concentration of ZnO NPs, as a consequence serum testosterone levels decrease as reported in Wistar Han rats (Hussein *et al.*, 2016). Additionally, the same authors explored the influence of ZnO NPs on steroidogenesis enzymes by assessing the levels of steroidogenic protein mRNA expression from testis samples, such as 3β-Hydroxysteroid dehydrogenase (3β-HSD), 17β-Hydroxysteroid dehydrogenases (17β-HSD) and steroidogenic factor 1 (Nr5A1). 3β-HSD and 17β-HSD (Hussein *et al.*, 2016). These are enzymes responsible for the conversion of pregnenolone, a cholesterol derivative, into progesterone and androstenedione, a progesterone derivative, in testosterone, respectively (Ewing and Zirkin, 1983). Nr5A1 is a transcription factor that regulates the expression of several steroidogenic enzymatic genes on Leydig cells (such as 3β-HSD and aromatase) and is involved in the steroidogenesis pathway and synthesis of testosterone (Payne and Hardy, 2007). The expression of mRNA steroidogenic proteins showed a significant decrease in ZnO NPs exposed groups, which justifies the lowering in serological testosterone levels (Hussein *et al.*, 2016).

As mentioned in previous studies, ZnO NPs is a source of oxidative stress due to their accumulation on liver. In order to evaluate antioxidant parameters in rats and mice, some studies analysed the activity of Superoxide Dismutase (SOD), Glutathione Peroxidase (GPx), Reduced Glutathione (GSH), Catalase (CAT) and Total Antioxidant Capacity (TAC). The levels of lipid peroxidation marker Malondialdehyde (MDA) and of Total Oxidant Status (TOS) were also assessed to evaluate the oxidative stress. A significant reduction in the activity of antioxidant enzymes (CAT, SOD, GPx) and of GSH (Hussein *et al.*, 2016), just as TAC was decreased in the blood sample of Wistar rats (Abbasalipourkabir *et al.*, 2015). TOS and the lipid peroxidation level have been shown to increase significantly after exposure to a high concentration of ZnO NPs (Abbasalipourkabir *et al.*, 2015; Hussein *et al.*, 2016). Thus, ZnO NPs may be considered an inhibitor of the antioxidant machinery and an oxidative stress inducer. Reduction in sperm viability occurs as a result of ROS formation in liver. ROS induce chromosomal alterations in blood samples and DNA damage, indicating that rats exposed to high concentration of ZnO NPs have higher levels of ROS in organism that induce apoptosis of sperm cell (Srivastav *et al.*, 2017).

Contrary to the majority of studies, sheep exposure to ZnO NPs improved the sperm parameters and neutralized the effects of ROS by increasing its antioxidant activity. These results are attributed to the zinc antioxidant activity and its role in the stabilization of sperm according with the study. According with authors, it is important to note that different animal species have differential nutritional needs for spermatogenesis, and until now no *in vivo* published study about the effect of ZnO NPs on spermatogenesis reported any animal model other than rodents. In addition, the dose of ZnO NPs is lower compared to other studies. Thus, future studies are needed to clarify these results, by repeat the study with higher doses of exposure (Abaspour Aporvari *et al.*, 2018).

1.6.2.2. *In vivo* studies in non-mammalian animal models

Non-mammalian *in vivo* studies have similar results to those obtained from mammalian *in vivo studies* research. In testis from Japanese quail treated with ZnO NPs, the morphology analysis of ST revealed a decrease in diameter and height of the

epithelium, as mammalian *in vivo* studies reported, that result from germ cell loss, and apoptotic effect of ZnO NPs on spermatogenic cells. Further, the testosterone serum levels decreased with exposure to ZnO NPs. In addition to the histological analysis of the Japanese quail testis, egg hatchability was also evaluated after sperm exposure to different concentrations of ZnO NPs, to assess the sperm functionality. In this way, the cytotoxic effects of ZnO NPs in sperm cell have repercussions in fertility, causing infertility and higher incidence of embryonic deaths, reducing hatchability rates and inducing teratogenic effects on their embryos. (Khoobbakht *et al.*, 2018). These results emphasize the importance of toxicity study in male germ cells, once ZnO NPs are capable to reduce the fertility from Japanese quail.

ZnO NPs exposure on germ cell apoptosis was also evaluated in *Caenorhabditis elegans*, reporting that this type of metal nanoparticles as apoptotic inducer in germ cells. Exposure of *C. elegans* to ZnO NPs caused an increase in apoptotic cell number, resulting from a change in apoptotic gene regulation. The apoptotic genes cep-1, cep-13, efl-2, egl-1, lin-35, and sir-2.1 were significantly upregulated in the presence of ZnO NPs, inducing cell apoptosis (O'Donnell *et al.*, 2017). Although, it is necessary to be aware that this animal model is hermaphrodite, in this study no distinction was made between germ cells. Thus, it is necessary study the expression of upregulated genes in male mammalian cells to better understand the apoptosis mechanism behind ZnO NPs in germ cells.

Objectives

2. Objectives

ZnO NPs are applied in a vast variety of biomedical applications and numerous studies have focused on biosafety of ZnO NPs, but there are few studies that determine its possible adverse effects on male reproductive health especially at male germ cells level. ZnO NPs are considered a dose and time dependent cytotoxic inducer in testis, Leydig cells, Sertoli cells, spermatocytes and sperm cells. Cell viability reduction occurs possibly because of ROS levels increase, DNA damage, lipid peroxidation and cell apoptosis, as recent studies reported. Their consequences on the first cell stage of spermatogenesis, the spermatogonia cells was not previously evaluated. Thus, the main objective of this dissertation is to know the consequences of ZnO NPs exposure on the first cell stage of spermatogenesis, the spermatogonia. For this is necessary:

- Understand and identify the contributions of recent toxicity studies in male reproductive system to comprehend the consequences of ZnO NPs exposure;
- Detect the main issues to be addressed based on the recent ZnO NPs toxicity studies in male reproductive system;
- Identify the toxic concentration and exposure time of ZnO NPs in spermatogonia cell line;
- Determine if short exposures to ZnO NPs induce alterations on spermatogonia;
- Evaluate the cytotoxic effects of ZnO NPs in spermatogonia cells;
- Assess the cytoskeleton and nuclear envelope alterations in spermatogonia cells upon exposure to ZnO NPs;

Materials and Methods

3. Materials and Methods

3.1. Characterization of Zinc Oxide Nanoparticles (ZnO NPs)

ZnO NPs (Aldrich) were kindly provided by Professor Ana Maria Senos and Professor Elisabete Costa (Department of Materials and Ceramics Engineering and CICECO-Aveiro Institute of Materials, University of Aveiro). All ZnO NPs characterization was also made by the referred Professors.

3.2. ZnO NPs concentrations and incubation times

Six different concentrations of ZnO NPs and two different incubation times were selected for the treatment of GC-1 spg cells (ATCC® CRL2053™). The concentrations and incubation periods points are indicated in Table 3.

Table 3: Concentrations and incubation times of ZnO NPs.

Incubation Time	ZnO NPs Concentrations (μg/ml)					
6 hours	0	1	5	8	10	20
12 hours	0	1	5	8	10	20

3.3. Characterization of GC-1 spg (ATCC® CRL2053™) cell line

GC-1 spg cells (ATCC® CRL2053™) or GC-1 are mouse-derived spermatogonial cell line. This cell line presents characteristics between type B spermatogonia and primary spermatocytes, and express two testis specific isoproteins, the cytochrome c and the lactate dehydrogenase C4. In culture, these cells exhibit an epithelial morphology and present adherent growth properties. They are cultured with Dulbecco's Modified Eagle's Medium (DMEM, bioWest) supplemented with 10% (v/v) of Fetal Bovine Serum (FBS, bioWest) and 1% (v/v) of penicillin-streptomycin mixture (Pen Strep, bioWest). Cells were incubated at 37°C in a humidified atmosphere of 5% CO_2 and of 95% O_2.

3.4. Preparation and sterilization of ZnO Nanoparticles for cell culture

ZnO NPs were reconstituted in sterile 1x PBS at a concentration of 2000 µg/ml and sonicated for 3 minutes set at 60% amplitude with cycles pulses of 1 second. From this suspension a stock solution of 200 µg/ml was performed using GC-1 cells complete growth medium. The stock solution was further sonicated for 3 minutes set at 60% amplitude with cycles pulses of 1 second, and then sterilized by UV radiation for 20 minutes. Subsequently, the different concentrations of ZnO NPs (Table 3) were prepared by diluting this stock solution.

3.5. Cell preparation for assays

GC-1 spg cells (ATCC® CRL2053™) were seeded at the density of $2{,}5x10^5$ cells per well in 6 well plates (Orange scientific) 16 hours before the incubation with ZnO NPs. Except for the ROS intracellular levels assay, where the cells were seeded onto black 96 well plates (4titude) at a density of $1x10^4$ cells/well for 16 hours. Upon that period GC-1 cells were treated with different ZnO NPs concentrations (0–20 µg/ml) for 6 and 12 hours (Table 3), previously prepared and sterilized for cell culture.

3.6. Cell Viability Analysis

The GC-1 cells viability was measured by using three different assays: resazurin, trypan blue and flow cytometry by annexin V APC and propidium iodide (PI), described below.

3.6.1. Resazurin Reduction Assay

Resazurin (7-hydroxy-10-oxidophenoxazin-10-ium-3-one) also called Alamar Blue, is a soluble faintly fluorescent blue dye. It is a cell permeable redox indicator, which can be enzymatically converted into resorufin, a pink and highly fluorescent dye (Rampersad, 2012; Uzarski *et al.*, 2017). This reaction is an inexpensive, simple and noninvasive colorimetric method for accessing cell viability according to metabolic activity (Uzarski *et al.*, 2017). This assay results from mitochondrial reductases secreted by cells namely, NADPH, FADH, FMNH and NADH, and from cytochromes, responsible for electron transfer

to resazurin, which are reduced to resofurin by NADH oxidation to NAD^+ (Figure 6). In addition, other enzymes such as the diaphorases (dihydrolipoamine dehydrogenase), NAD(P)H: quinoneoxidoreductase and flavin reductase are able to reduce resazurin (Rampersad, 2012).

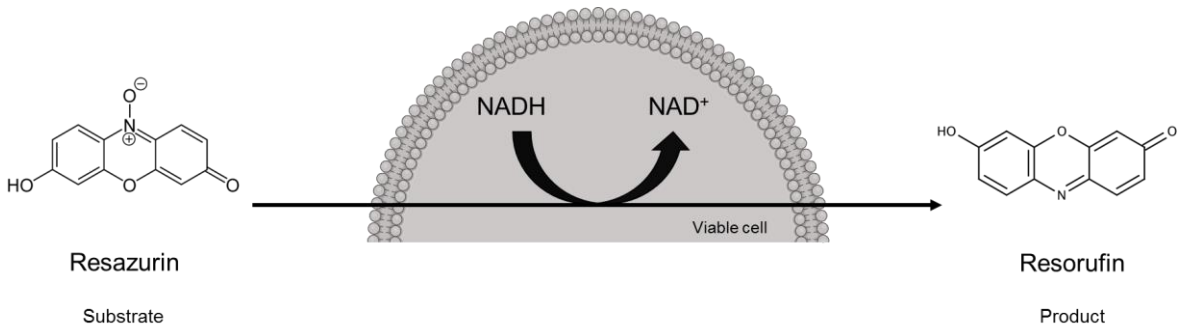

Figure 6: Structure of resazurin substrate and the resorufin product resulting from reduction by oxidation of NADH into NAD^+ by viable cells. NAD- Nicotinamide Adenine Dinucleotide (Adapted from: *Riss et al. 2016*).

Absorbance measurements were made using an absorbance reader (Infinite M200 PRO, Tecan). The optical density of resofurin and resazurin were measured at 570nm and 600nm wavelengths, respectively, and the ratio between the two is given by (Ri=O.D.570nm/ O.D.600nm) (Pina *et al.*, 2010). Thus, the higher optical density of the product and the lower the reaction substrate, the bigger is Ri, that corresponds to the metabolic activity of cell and, consequently, highest cell viability. In Ri, the ratio of the cell-free medium (R0) of each different concentration of ZnO NPs, is subtracted to give Rf (Pina *et al.*, 2010).

Rf was measured in GC-1 cells treated with different ZnO NPs concentrations (0–20 µg/ml) for 6 and 12 hours. Resazurin was prepared at a concentration of 0,10 mg/ml in 1x PBS and its pH adjusted to 7.4 before being sterilized by filtration. Therefore, during exposure to ZnO NPs, 10% of resazurin sodium salt (Sigma-Aldrich) in DMEM medium solution was added to the cells 4h before the end of exposure to nanoparticles. The optical density reading was made in 96 well plates, after 100µL of cell culture medium from all conditions was collected to microplate. The optical density of fresh culture

medium with different concentrations of ZnO NPs were also measured to access R0. Absorption results were normalized to achieve Rf.

3.6.2. Trypan Blue analysis

Trypan blue is a blue dye exclusion method that recognizes two cell populations according to membrane integrity, the live and death cells. Live cells have intact cell membranes that exclude trypan blue, whereas dead cells do not, presenting a blue cytoplasm. The dye exclusion technique provides a simple and rapid test to access cell viability by counting the number of clear and blue cells, that correspond to viable and unviable cells, respectively (Strober, 2019).

The number of viable and dead cells was evaluated using 0.4% Trypan blue solution and a haemocytometer. The GC-1 cells were incubated with different concentrations of ZnO NPs for 6 hours and 12 hours (Table 3). Medium was collected, and cells were resuspended and centrifugated for 3 minutes at 1000 rpm before incubating with Trypan blue for 1 minute. Viability was assessed as a ratio of viable cells to the total number of cells.

3.6.3. Flow Cytometry evaluation by Annexin V APC and Propidium Iodide, markers of apoptosis and necrosis respectively

Apoptosis and necrosis are the two main forms of cell death. Apoptotic cells undergo some changes in the structure of their plasma membrane, one of these alterations is the exposure of phosphatidylserine (PS) to the outer surface of the membrane, which is usually found in the intracellular leaflet, facing cytosol. PS flipping to the external cell surface occurs well before the integrity of the plasma membrane is compromised. (Darzynkiewicz *et al.*, 1992; Reutelingsperger and Heerde, Van, 1997; Vermes *et al.*, 1995). Annexin V is a Ca^{2+} dependent phospholipid-binding protein that can be used for apoptosis detection given that it binds with high affinity and specificity to PS. It can differentiate early apoptotic cells, although it does not distinguish late apoptotic cells from necrotic cells. Therefore, measurement of Annexin V binding should be performed in conjunction with PI, a dye exclusion test that evaluates the integrity of the

cell membrane. In viable and early apoptotic cells, the cell membrane excludes PI as it remains intact. While in late apoptotic and necrotic cells the integrity of cell membrane is lost, PI can cross the membrane cell to the nucleus where it binds to DNA, producing a strong red fluorescence (Demchenko, 2013; Reutelingsperger and Heerde, Van, 1997; Vermes *et al.*, 1995).

Conjugated recombinant Annexin V (Annexin V APC- ImmunoTools) and the PI were used as apoptosis and necrosis markers, respectively. For flow cytometry, GC-1 cells and medium were collected after 6 hours and 12 hours of exposure to 0, 5, 10 and 20 µg/ml of ZnO NPs. For positive control the cells were treated with H_2O_2 for 2 hours at a concentration of 100 mM. The cells suspensions were centrifuged at 1000 rpm for 3 minutes at 4ºC and the cell pallet was resuspended in binding buffer (1x PBS with Ca^{2+} at a concentration of 0,33 g/L), before being centrifuged again and resuspended with annexin V APC diluted in binding buffer. Cells were exposed to annexin V APC during 15 minutes in the dark. Prior to cytometry analyses BD Accurati™ C6 Software (BD Biosciences®), the cells were exposed to a new centrifugation procedure and resuspended again in binding buffer, the PI was added at a final concentration of 100 µg/ml. For controls, the cytometry analysis was performed first with annexin alone and, at the end, PI was added, and new flow cytometry analysis was performed, except for negative control, which was not incubated with annexin V APC and PI.

3.7. Cell damage evaluation

3.7.1. Evaluation of intracellular ROS levels

Reactive species analysis is difficult in part because of their short lifetime, and the variety of antioxidants *in vivo*. 2,7-dichlorodihydrofluorescein diacetate (DCFH-DA) has been used for detecting several Reactive Oxygen Species (ROS) and Reactive Nitrogen Species (RNS) in biological media, providing a sensitive and rapid quantification of reactive species. It can be applied in cell studies due to its ability to diffuse through the cellular membrane and accumulate in cytoplasm. Intracellular esterase's first hydrolyse the non-fluorescent lipophilic probe DCFH-DA to non-fluorescent 2,7-dichlorodihydrofluorescein (DCFH), which is then oxidized by reactive species and

originates 2,7-dichlorofluorescein (DCF), a fluorescent compound (Figure 7) (Gomes, Fernandes and Lima, 2005; Halliwell and Whiteman, 2004; Pavelescu, 2015; Possel *et al.*, 1997).

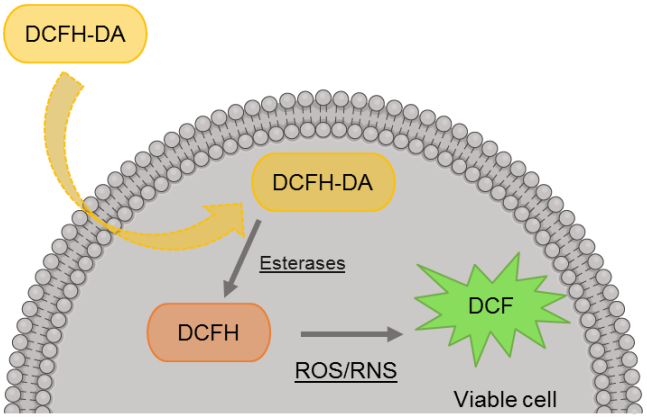

Figure 7: Schematic representation of the mechanism of 2,7-dichlorodihydrofluorescein diacetate (DCFH-DA) action within the cells. DCFH: 2,7-dichlorodihydrofluorescein; DCF: 2',7'-Dichlorofluorescein. (Adapted from: *Halliwell and Whiteman, 2004; Pavelescu, 2015*).

In order to detect intracellular ROS levels, DCFH-DA green fluorescence was monitored in GC-1 cells using the Total ROS Detection kit (ENZO Life Sciences). Cells were incubated with 0, 5, 10 and 20 µg/ml of ZnO NPs for 6 hours and 12 hours (Table 3). One hour before the end of ZnO NPs treatments, ROS detection solution was added to each condition. For negative control, the ROS inhibitor, N-acetyl-L-cysteine (NAC), was incubated 30 minutes before the ROS detection solution. Finally, for positive control the ROS inducer (Pyocyanin) was incubated 30 minutes after the addition of ROS detection solution. For the background assessment, cells for each condition (Table 3) without ROS detection solution were also prepared. At the end of incubation, the fluorescein intensity, with fluorescence excitation and emission 488 and 520, respectively was measured without removing the detection mixture under a fluorescence microplate reader (Infinite M200 PRO, Tecan). Results were normalized using the corresponding background reading.

3.7.2. DNA damage evaluation

The levels of DNA damage were assessed by detection of γ-H2AX (S139) intracellular levels by immunoblotting. γ-H2AX is a marker of DNA repair and of DNA double-strand breaks (Solier and Pommie, 2014).

3.8. Protein levels analysis

3.8.1. Protein Collection and Quantification

Cell lysates from GC-1 cells incubated for 6 and 12 hours with different concentrations of ZnO NPs (Table 3), were collected in 1% Sodium dodecyl sulfate (SDS) solution and then boiled at 95ºC for 5 minutes. SDS is an anionic charged detergent that provide cell lysis by denaturing cell proteins (Brown and Audet, 2008; Peach *et al.*, 2015) Then, lysates were sonicated for 5 seconds, set at 60% amplitude with cycles pulses of 0,5 second.

Total protein from cellular lysates content was quantified by Pierce's bicinchoninic acid (BCA) protein assay kit (Thermo Scientific) using an absorbance reader. This kit provides a colorimetric detection and quantification of total proteins based on reduction of Cu^{2+} to Cu^{+} by proteins. Cu^{+} interacts with BCA which forms an intense purple-coloured reaction product that can be measured at 562 nm. The purple product is proportional to the amount of Cu^{+} that is equivalent to protein the concentration. To achieve the protein concentration, the bovine serum albumin (BSA) was used as a reference standard. The concentration of each unknown sample was determined based on the standard curve established in accordance with concentrations of BSA (Smith *et al.*, 1985).

3.8.2. SDS-PAGE, Immunoblotting and Total Protein Detection

Protein samples were separated according to their molecular weight on a 5-20% gradient SDS polyacrylamide denaturing gel electrophoresis (SDS-PAGE) using a 90mA electrical current to the gel for 3/4 hours. 40µg of protein samples were boiled for 10 minutes with 1x loading buffer (LB) before loading. A precision plus Protein ™ Dual Colour Standards molecular weight marker (Bio-Rad) was loaded into the gradient gel.

Additionally, the immobilized proteins were subsequently electrotransferred into a nitrocellulose membrane (pore size 0.2 µm; Whatman) for 18 hours at 200 mA. The total amount of protein content on the nitrocellulose membrane was detected by ponceau S reversible staining (Sigma-Aldrich), which was incubated for 5 minutes and then scanned on a GS-800 calibrated image densitometer (Bio-Rad). Membranes were washed with 1x TBS-T for complete removal of Ponceau S solution. Nitrocellulose membranes were blocked for 4 hours to prevent non-specific binding of primary antibodies with 5% BSA/ 1x TBS-T. Primary antibodies used were (Table 4): the mouse anti-γ-H2AX (S139); mouse anti-β-tubulin; mouse anti-β-actin; mouse anti-α-tubulin-acetylated and rabbit anti-SUN1 and were all incubated overnight at 4 °C. The secondary antibodies used were: the anti-mouse and rabbit horseradish peroxidase conjugated (Table 5), which were incubated for 2 hours at room temperature. After incubations with primary and secondary antibodies, the membranes were washed for 1 hour with 1X TBS-T, during 10 minutes between washes. Finally, to detect protein bands, the ECL™ Select WB detection reagent (GE Healthcare) was incubated for 5 minutes into nitrocellulose membranes. These bands were scanned and quantified (GS-800™ Calibrated Densitometer and Quantity One densitometry software, Bio-Rad), and immunoblot data normalized for the respective ponceau loading control.

Table 4 : Primary antibodies used and their respective target proteins. The dilution used depends on the assay. BSA - Bovine Serum Albumin; PBS - Phosphate-buffered saline solution; TBS-T - Tris-buffered saline-Tween; ICC - Immunocytochemistry; WB - Western Blot.

Primary Antibody	Description	Origin/Suplier	Dilution	Blocking Solution	Target
Anti-γ-H2AX (S139)	Mouse, monoclonal	Millipore	WB: 1:500	3% BSA / 1x TBS-T	γ-H2AX (S139)
Anti-β-Tubulin	Mouse, monoclonal	Invitrogen Life technologies	WB: 1:1000 ICC: 1:500	3% BSA/ 1x TBS-T 3% BSA/ 1x PBS	β-Tubulin
Anti-β-Actin	Mouse, monoclonal	Sigma-Aldrich	WB: 1:5000	3% BSA/ 1x TBS-T	β-Actin
Anti-α-Tubulin acetylated	Mouse, monoclonal	Sigma-Aldrich	WB: 1:2000 ICC: 1:250	3% BSA/ 1x TBS-T 3% BSA/ 1x PBS	α-Tubulin acetylated
Anti-Sun1	Rabbit	kindly provided by our collaborator	WB: 1:2000	3% BSA/ 1x TBS-T	Sun1

Table 5: Secondary antibodies. The dilution used depends on the assay. BSA - Bovine Serum Albumin; PBS - Phosphate-buffered saline solution; TBS-T - Tris-buffered saline-Tween; ICC - Immunocytochemistry; WB - Western Blot.

Secondary Antibody	Description	Origin/Suplier	Dilution	Blocking Solution
Anti-mouse	Horse, anti-mouse	Cell Signalling Technology	WB: 1:10000	5% BSA/ 1x TBS-T
Anti-rabbit	Goat, anti-rabbit	Cell Signalling Technology	WB: 1:10000	5% BSA/ 1x TBS-T
Alexa Fluor 488	Goat, anti-mouse	Life Technologies	ICC: 1:300	3% BSA/ 1x PBS

3.8.3. Immunocytochemistry and microscope analysis

Immunocytochemistry (ICC) allows to visualize, through protein-antibody interactions, the relative abundance of a specify protein or antigen in cells and their subcellular localizations, under fluorescence microscopy. In indirect detection used in this

assay, the primary antibody target the molecule of interest and a labelled secondary antibody, that has a conjugated fluorophore, is directed against the constant region of the primary antibody. (Griffiths, 2012; Novus Biologicals, 2015).

GC-1 were treated with fresh media containing 0 and 20 µg/ml of ZnO NPs for 6 hours and 12 hours. The samples were fixed in 3,7% formaldehyde and then permeabilized with 0,2% Triton X-100. Additionally, cells were blocked with 3% BSA in 1x PBS and were incubated with primary antibodies for β-tubulin and acetylated α-tubulin (Table 4) for 2 hours, followed by secondary antibody (Table 5) and fluorophore-labelled phalloidin dye (Alexa Fluor 568 phalloidin, molecular probes, 1:500) for 1 hour. Between all these steps, fixation, permeabilization and antibodies incubation, cells were washed with 1X PBS. Finally, the coverslips were mounted on a microscope slide with 4',6-diamidino-2-phenylindole (DAPI)-containing VECTASHIELD® Mounting media (Vector Laboratories). Cytoskeleton were counterstained with phalloidin and nuclei the with DAPI dyes which binds to F-actin and DNA, respectively. Phalloidin emits red-orange fluorescence, whereas DAPI emits blue light (Novus Biologicals, 2015). Preparations were visualized using an LSM880 (Zeiss) confocal microscope and a 63x/1.4 oil immersion objective. Microphotographs were acquired in a sole section in the Z-axis and represent a mean of 10 scans. Fluorescence intensity analyses of β-tubulin, acetylated α-tubulin and F-actin staining were performed using ImageJ software (U. S. National Institutes of Health). The fluorescence intensity from at least 30 cells per condition was acquired according with the corrected total cryosection fluorescence (CTCF) formula, that is calculated as (CTCF = Integrated density - (area of selected cell × mean fluorescence of background)).

3.9. Treatment of results and statistical analysis

Results were expressed as the ratio (%) of the data from ZnO NPs treated cells per the data from ZnO NPs untreated cells (0 µg/ml of ZnO NPs), for each time point. The proportion was calculated using Excel. All trials were carried out in at least three independent experiments with two replicates per assay, for each condition. Statistical analysis was performed by GraphPad (GraphPad Prism version 6.00 for Windows), using Two-way ANOVA followed by Dunnett's multiple comparisons test with a statistical

confidence coefficient of 0.95, for comparisons between time points and concentrations. One-way ANOVA was used, followed by the Dunnets test with a statistical confidence coefficient of 0.95, for comparisons between concentrations per time-point. All data were expressed as mean ± standard error of the mean.

Results

4. Results

4.1. ZnO NPs reduce the viability of GC-1 in a dose and time dependent way

Given previous studies, ZnO NPs has been described as a toxic factor that affect different cell types, including cells from male reproductive system, namely spermatocytes (Liu *et al.*, 2016), spermatozoa (Barkhordari *et al.*, 2013), Sertoli cells (Han *et al.*, 2016; Liu *et al.*, 2016) and Leydig cells (Han *et al.*, 2016). However, spermatogonia cells exposure to ZnO NPs were not evaluated until now. Of note, the periods of incubation selected for this study were considerable low to minimize exposure to different amounts of ZnO NPs. The objective is to determine if these short exposure to ZnO NPs in fact induce alterations on spermatogonia.

In order to investigate the effects of ZnO NPs on cellular metabolic activity and on cell membrane integrity of mouse spermatogonia cells, GC-1 cells incubated with different concentrations of ZnO NPs for 6 and 12 hours was assessed using two different viability assays, resazurin assay and trypan blue exclusion method, respectively. According to results from resazurin assay (Figure 8A), the cell viability significantly decreased after 6 hours incubation with 10 µg/ml ($p < 0,01$; $p \leq 0,001$) and 20 µg/ml ($p \leq 0,001$; $p < 0,0001$) corresponding to a cell viability decrease of 13% and 17%, respectively. Upon 12 hours of ZnO NPs exposure, the cell viability was only altered at a ZnO NPs concentration of 20 µg/ml ($p<0,0001$), decreasing 48% when compared with control (ZnO NPs unexposed cells for 12 hours). Moreover, using the second viability approach (trypan blue exclusion method) the results were quite similar (Figure 8B). However, cell viability only decreased significantly using the higher ZnO NPs concentration (20 µg/ml) for either 6 hours ($p \leq 0,001$; $p < 0,05$) or 12 hours ($p < 0,0001$).

Viability decrease is associated with an increase in cell death. To assess the mechanism of cell death, GC-1 were treated with 0, 5, 10 and 20 µg/ml of ZnO NPs for 6 hours and 12 hours and the apoptotic and necrotic cells were analysed by flow cytometry, as previously described in material and methods section 3.7.2. Necrotic cells and early apoptotic cells were stained with PI and annexin V APC, respectively. The exhibition of both dye markers at cell surface, represents a sign of late apoptotic cells. For this study,

necrotic and late apoptotic cells were accounted together because in both type of cell death, cells loss their membrane integrity in a gradual process. The results indicated a significant increase in number of late apoptotic and necrotic cells at an exposure dose of 20 µg/ml ZnO NPs for 12hours ($p < 0,01$) (Figure 8C). Thus, high concentrations of ZnO NPs can induce both apoptosis and necrosis of GC-1 cells. Given these cell viability alterations observed, the characterization of the type of damage induced by ZnO NPs in GC-1 cells was performed.

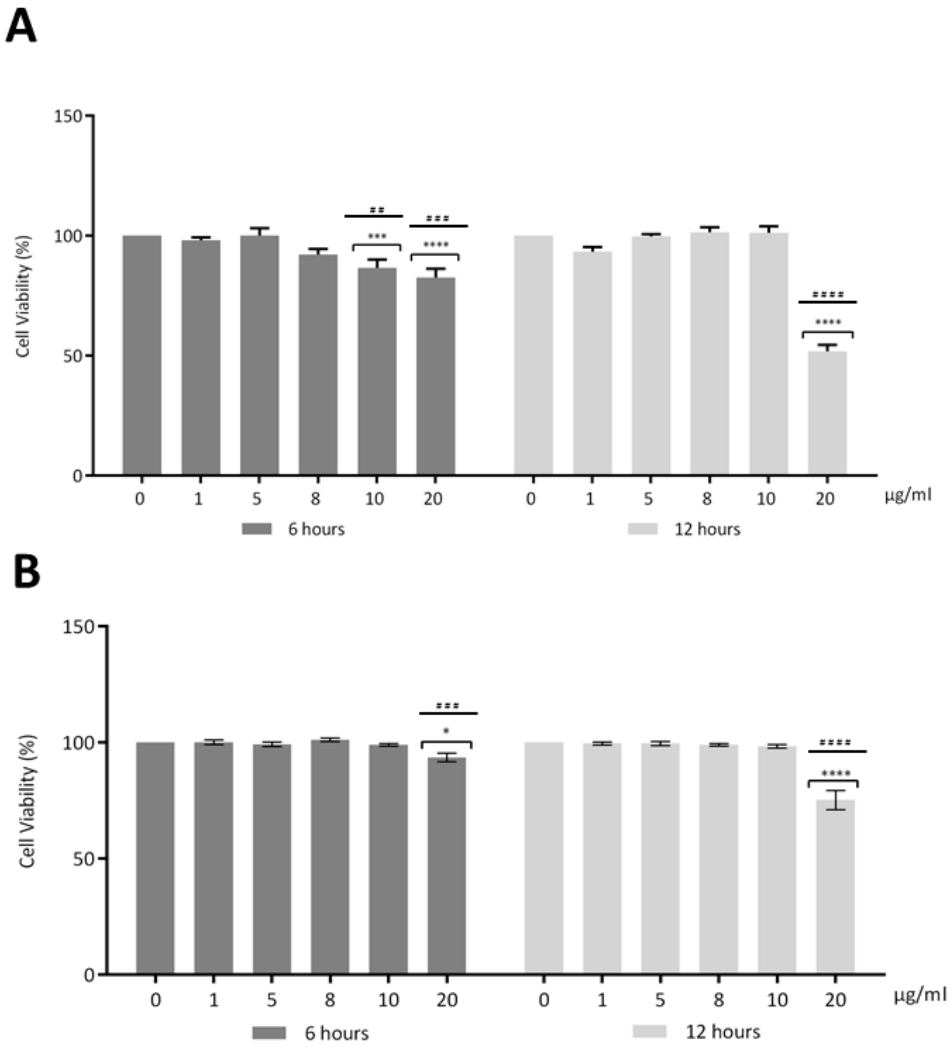

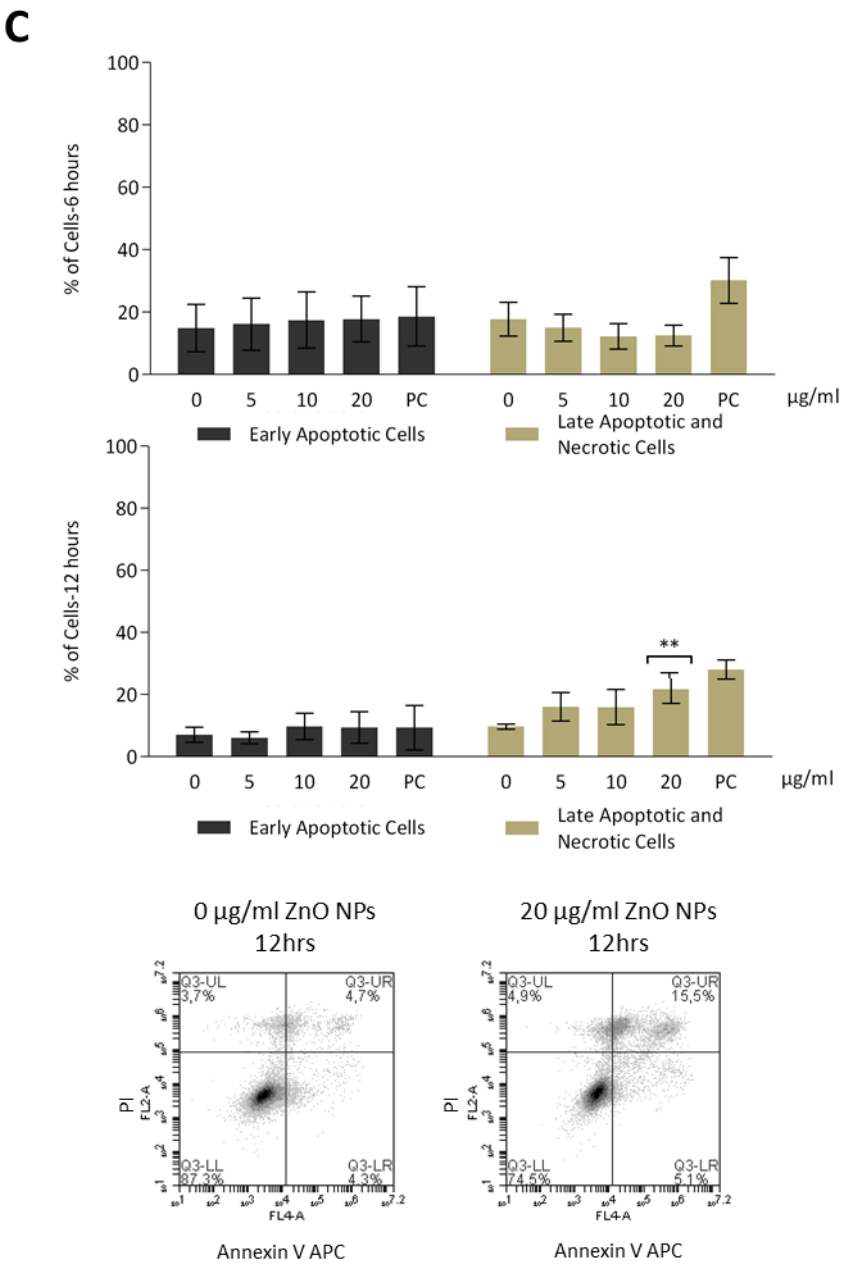

Figure 8: Evaluation of cell viability: A) Resazurin assay. Results from viability analysis of GC-1 spg (ATCC® CRL2053™) cell line after exposure for 6 hours and 12 hours to different concentrations of ZnO NPs. The percentage of viable cells was accessed by the resazurin assay. The percentage for each condition is presented as mean ± SEM of seven independent experiments. **B**) Trypan blue exclusion method. Trypan blue analysis of GC-1 spg (ATCC® CRL2053™) cell line after exposure for 6 hours and 12 hours to different concentrations of ZnO NPs. The percentage of viable cells was accessed by the trypan blue exclusion method. The viability percentage for each condition is presented as mean ± SEM of six independent experiments. **C**) Apoptotic and Necrotic Cell Death. Flow Cytometry data with Annexin V APC and PI membrane markers of GC-1 spg (ATCC® CRL2053™) cell line after exposure to 0, 5, 10, 20 µg/ml of ZnO NPs, for 6 hours and 12 hours. The percentage of apoptotic and necrotic cells was plotted as mean ± SEM of four

independent experiments. *for comparisons between concentrations and between time points, using two-way ANOVA. # for comparisons between concentrations, using one-way ANOVA. */# p <0,05. **/# # p <0,01. *** / # # # p ≤0,001. ****/# # # # p <0,0001. PI-Propidium Iodide.

4.2. Evaluation of Cell damage induced by ZnO NPs

4.2.1. ROS intracellular levels increase (oxidative damage)

Several studies reported the increase of ROS production as the cause of cytotoxicity by the exposure to ZnO NPs (Han *et al.*, 2016; Liu *et al.*, 2016). Therefore, to evaluate if ZnO NPs induce ROS levels alterations GC-1 cell line, ROS intracellular levels were assessed using the total ROS detection kit after incubation with 0, 5, 10 and 20 μg/ml of ZnO NPs for 6 and 12 hours (Figure 9A). GC-1 exposure to ZnO NPs (20 μg/ml) for 6 hours significantly increased ROS production comparing with control group (p <0,05). At 12 hours a significant alteration of ROS production levels was detected in cells presented to 5 (p <0,05), 10 (p <0,05, p <0,01) and 20 μg/ml (p <0,05) of ZnO NPs. However, the highest level of ROS does not correspond to the maximum concentration of ZnO NPs (20 μg/ml), as expected. From these results, high ZnO NPs concentrations and high exposure times to these NPs were associated with higher ROS levels.

4.2.2. DNA damage induction

Further, several studies indicated that ROS levels increase has been reported as the cause of DNA damage in cell lines exposed to ZnO NPs (Buzea, Pacheco and Robbie, 2007; Han *et al.*, 2016; Liu *et al.*, 2016). In the present study DNA damage was assessed through detection of γ-H2AX (S139) intracellular levels by immunoblotting. γ-H2AX is a marker of DNA double-strand breaks (Solier and Pommie, 2014) (Figure 9B). GC-1 cells exposed to different doses of ZnO NPs for 6 and 12 hours shown an increase of γ-H2AX (S139) in a dose and time dependent way. This rise was significant at 20 μg/ml after 6 hours of exposure (p <0,05) and highly significant at 20 μg/ml after 12 hours of treatment (p <0,01; p ≤0,001). Therefore, the exposure to higher concentration tested of ZnO NPs is a genotoxic factor by inducing DNA damage in GC-1 cell line. Ponceau S staining was used

as a loading control, as previously described. Given the alterations observed in GC-1 cells upon short time exposure to different concentrations of ZnO NPs the cytoskeleton alterations were subsequently investigated. Essentially, the levels of β-tubulin, acetylated α-tubulin (microtubules stabilization), β-actin and F-actin (actin remodelling) were assessed. Further the nucleoskeleton was also analysed through the levels of SUN-1 a member of the Linker of Nucleoskeleton and Cytoskeleton (LINC) complex (Figure 10 and Figure 11).

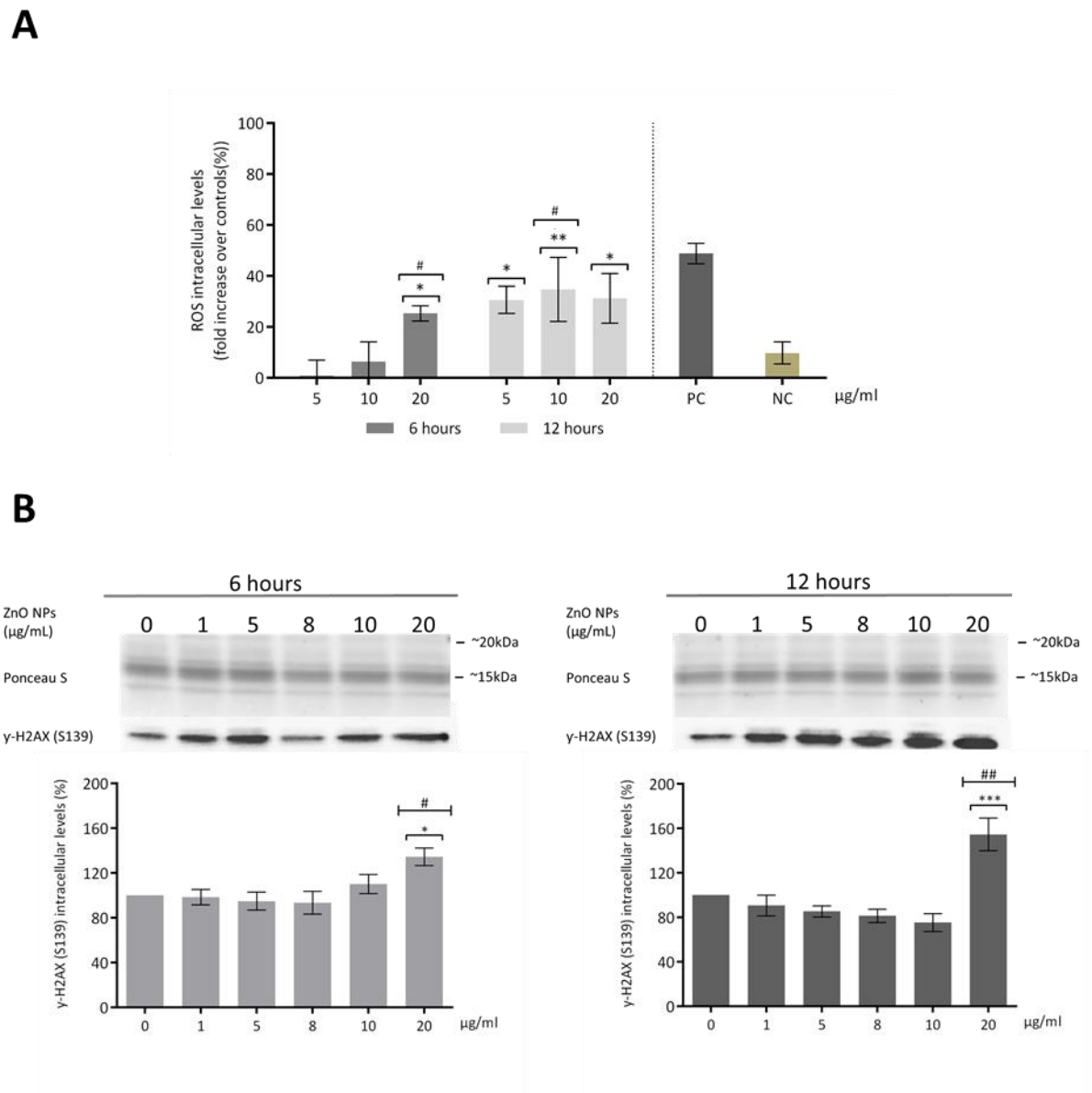

Figure 9: Cell damage induced by ZnO NPs. A) Oxidative Damage. ROS intracellular levels detection using the Total ROS Detection kit (ENZO Life Sciences) after the exposure of GC-1 spg cell line to different concentrations of ZnO NPs. The ROS levels were plotted as fold

increase over the control (cells without ZnO NPs) for both 6 hours and 12 hours. The values (%) for each condition were presented as a mean ± SEM of four independent experiments. **B)** DNA damage. Analysis of γ-H2AX (Ser 139), a repair marker of DNA damage, by immunoblotting in GC-1 spg cell line treated with different concentrations of ZnO NPs for 6 and 12 hours. Protein levels are presented as a fold increase (%) which was plotted as mean ± SEM of four independent experiments. *for comparisons between concentrations and between time points, using two-way ANOVA followed. # for comparisons between concentrations, using one-way ANOVA. */# p <0,05. **/# # p <0,01. *** p ≤0,001. ROS- Reactive Oxygen Species.

4.3. ZnO NPs influence Cytoskeleton and Nucleoskeleton dynamics in GC-1 cells

Previous studies described the ZnO NPs as a cause of cytoskeletal dynamic alterations in different types of cells but not spermatogonia (Choudhury *et al.*, 2017; García-Hevia *et al.*, 2016; Liu *et al.*, 2017). Therefore, the evaluation of the cytoskeleton integrity and dynamics was monitored in GC-1 cells upon their exposure to different concentrations of ZnO NPs for 6 and 12 hours. The β-tubulin levels decreased in a ZnO NPs dose dependent way after 12 hours of NPs exposure (Figure 10A). This decrease was only significant for the higher concentration of ZnO NPs tested (p ≤0,01; p ≤0,001). Moreover, no alterations of β-tubulin comparatively to control were noted after 6 hours of GC-1 exposure to ZnO NPs (Figure 10A). Significant alterations on acetylated α-tubulin levels (microtubules stabilization) after GC-1 exposure to ZnO NPs was observed. For acetylated α-tubulin the alterations were significantly increased when GC-1 cells were incubated with 20 μg/ml of ZnO NPs for both exposure periods (Figure 10B), at 6 hours (p<0,01; p<0,0001) and at 12 hours (p ≤0,001). No significant alterations at β-actin intracellular levels was verified by immunoblot (Figure 10C). However, a slight progressive increase dependent of dose is verified at 6 hours of incubation. Ponceau S staining was used as a loading control, as previously described.

Recent reports stated that ZnO NPs can induce cytoskeleton alterations that destroy the dynamic of cell. These changes in cytoskeleton can influence the structure of nucleoskeleton (Choudhury *et al.*, 2017). In order to identify possible alterations in nucleoskeleton at spermatogonia level, Sun1, an inner nuclear envelope protein of LINC complex (Pereira *et al.*, 2019), was monitored by immunoblot. The Sun1 intracellular levels significantly decrease after 6 hours of exposure to 8 (p <0,05; p <0,01), 10 (p <0,01;

p ≤0,001) and 20 µg/ml (p <0,01) of ZnO NPs and after 12 hours to 5 (p <0,01), 8 (p <0,01), 10 (p <0,05; p ≤0,001) and 20 µg/ml (p <0,05) (Figure 10D). Thus, ZnO NPs exposure not only affects the cytoskeleton, but also the nuclear envelope.

Given that β-tubulin and acetylated α-tubulin protein levels detected by immunocytochemistry change after GC-1 cells exposure to 20 µg/ml of ZnO NPs for 6 and 12 hours (Figure 11). Furthermore, the actin dynamics of GC-1 cells were monitored by F-actin, a specific marker of actin polymerization. β-tubulin (p ≤0,001) and F-actin (p<0,0001) increased significantly after 6 hours of ZnO NPs exposure. Although, after 12 hours, GC-1 cells presented a significant reduction of β-tubulin (p<0,0001) F-actin (p<0,0001), relatively to control cells. Moreover, at 6 hours of ZnO NPs treatment GC-1 cells showed an increase of acetylated α-tubulin levels (p ≤0,001), an indirect measure of microtubules stabilization. Similarly, after 12 hours of ZnO NPs exposure acetylated α-tubulin levels increased significantly (p <0,01), although were not so evident as after 6 hours.

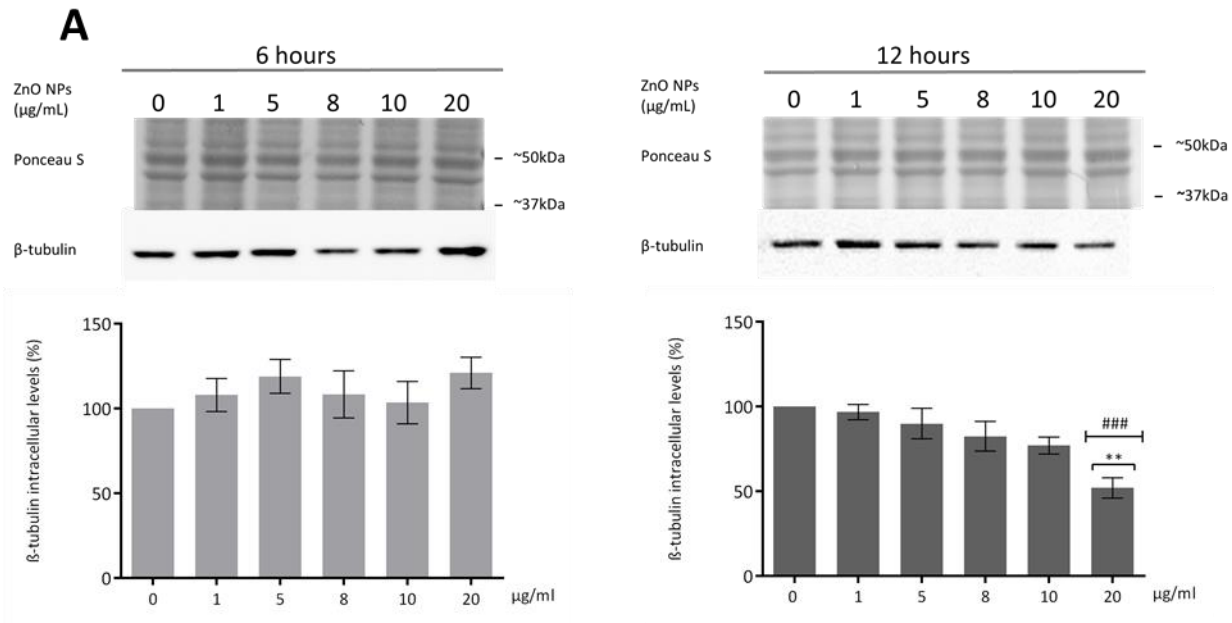

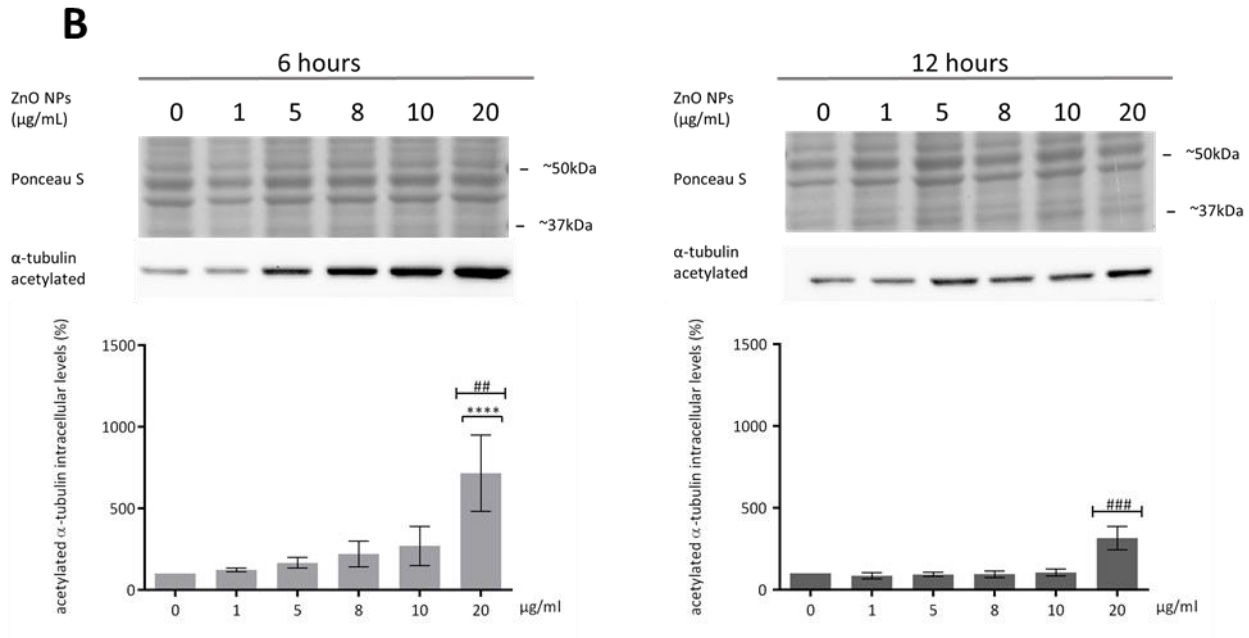
B
6 hours
12 hours
ZnO NPs (µg/mL)
0 1 5 8 10 20
Ponceau S
~50kDa
~37kDa
α-tubulin acetylated
acetylated α-tubulin intracellular levels (%)
1500
1000
500
0
##
****
###
µg/ml

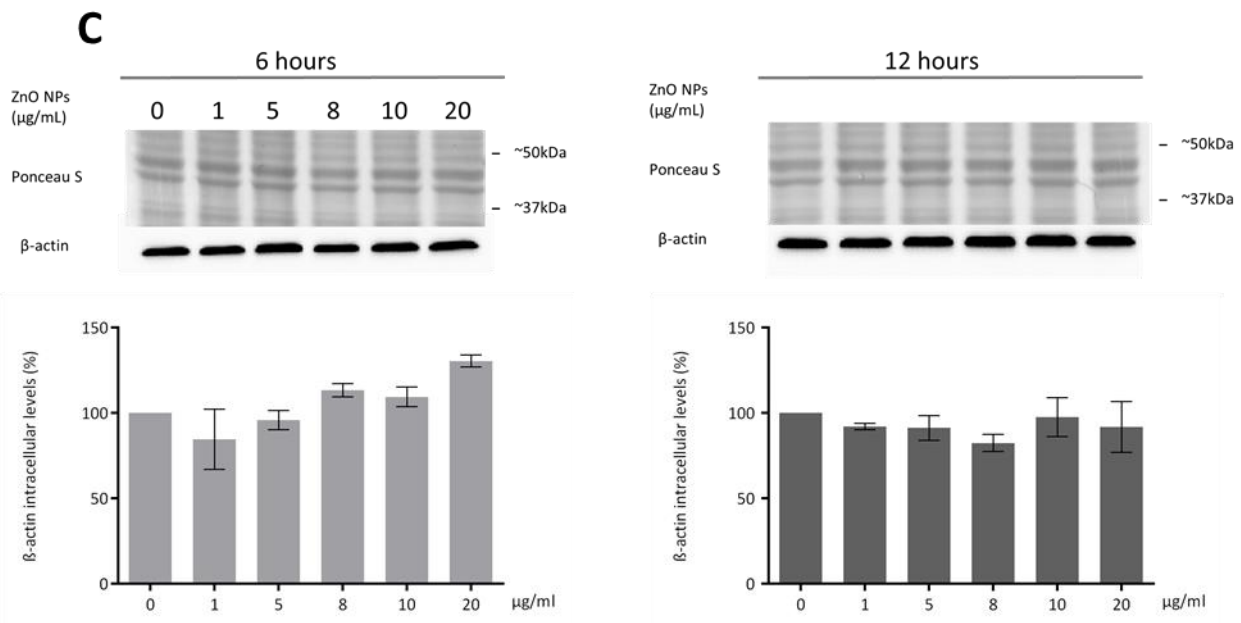
C
6 hours
12 hours
ZnO NPs (µg/mL)
0 1 5 8 10 20
Ponceau S
~50kDa
~37kDa
β-actin
β-actin intracellular levels (%)
150
100
50
0
µg/ml

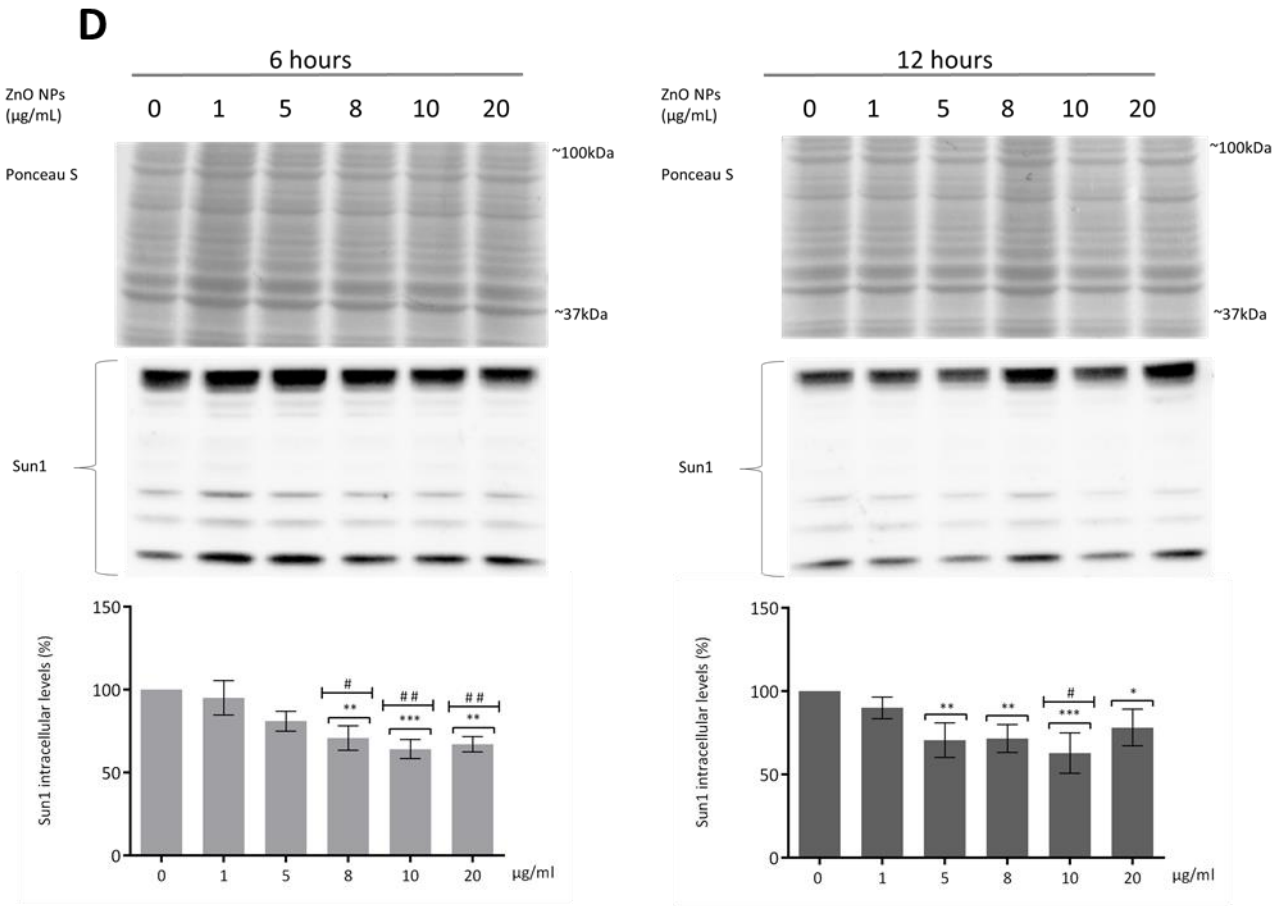

Figure 10: Influence of ZnO NPs in cytoskeleton and nucleoskeleton structure of GC-1 spg cell line, a quantification analysis by immunoblotting.

Cytoskeleton and Nucleoskeleton dynamics. Quantification of β-tubulin **(A)**, α-tubulin acetylated **(B)**, β-actin **(C)** and Sun1 **(D)** protein levels in GC-1 spg cell line by WB analysis. Cells were exposed to ZnO NPs for 6 hours and 12 hours. Protein levels are presented as a fold increase (%) which was plotted as mean ± SEM of four independent experiments, except the analysis of β-actin and Sun1 levels that was made in three independent experiments. *for comparisons between concentrations and between time points, using two-way ANOVA. # for comparisons between concentrations, using one-way ANOVA. */# p <0,05. **/## p <0,01. ***/### p ≤0,001. **** p<0,0001.

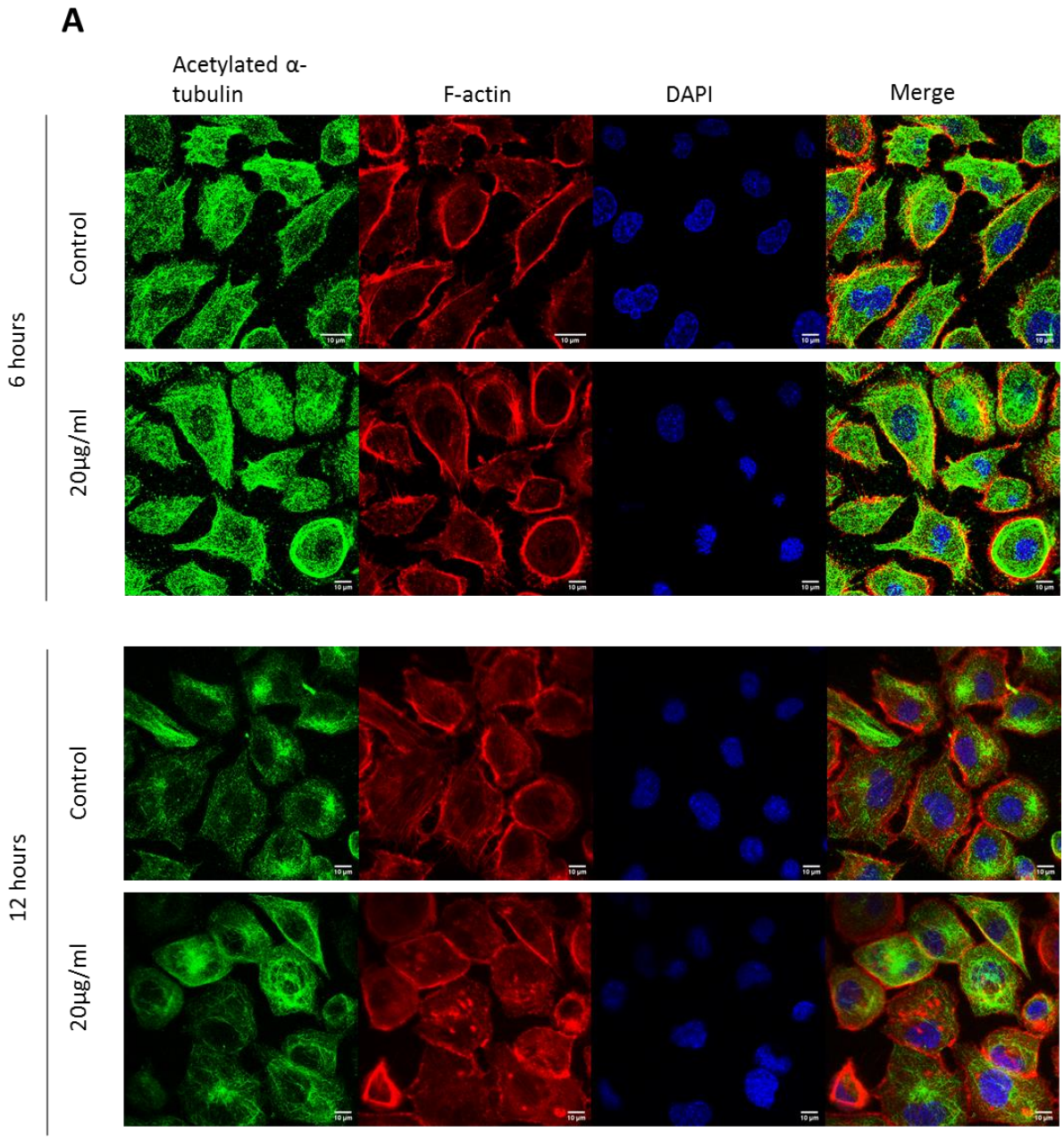
A
Acetylated α-tubulin
F-actin
DAPI
Merge
6 hours
Control
20µg/ml
12 hours
Control
20µg/ml

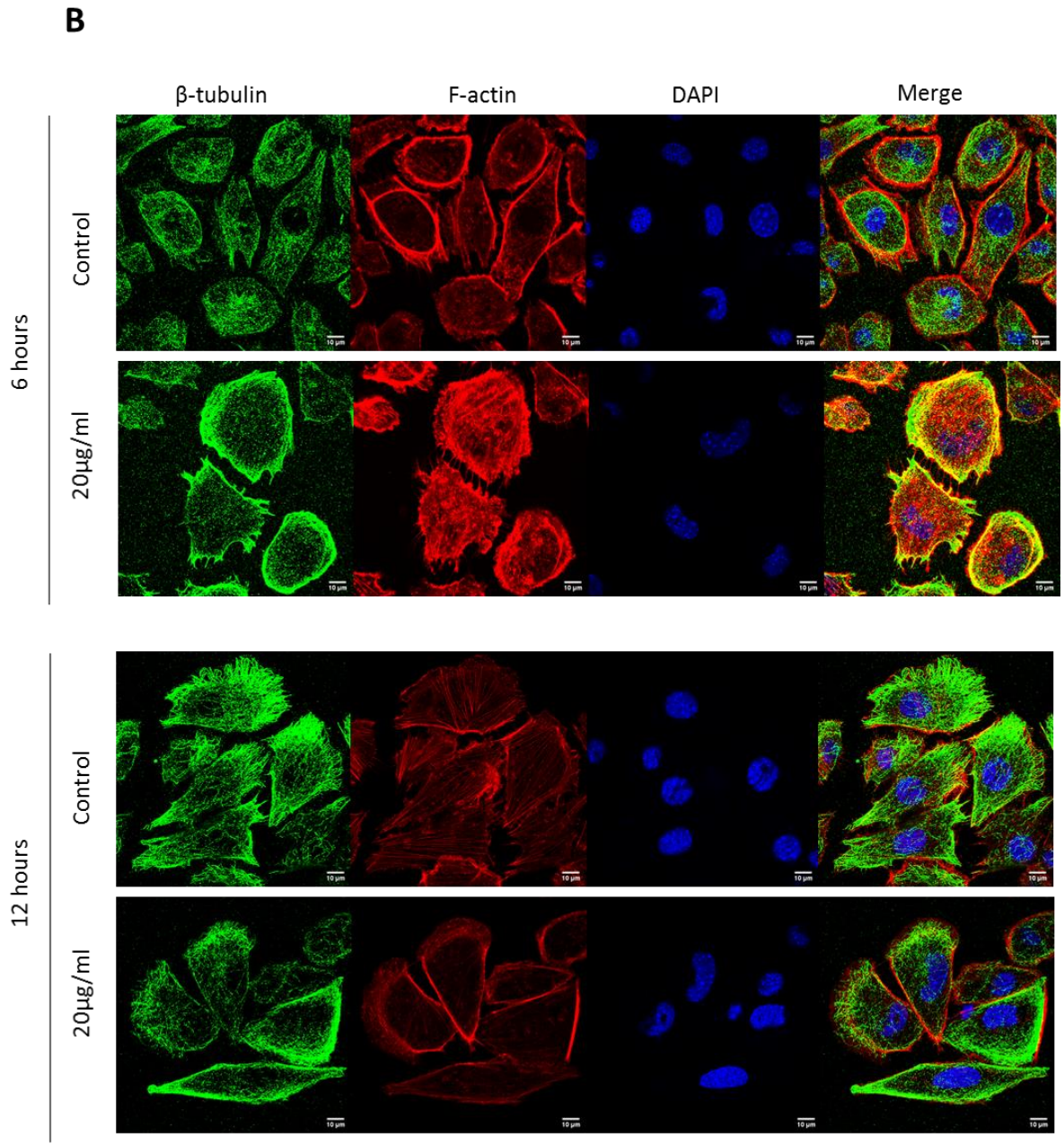
B
β-tubulin
F-actin
DAPI
Merge
6 hours
Control
20µg/ml
12 hours
Control
20µg/ml

C

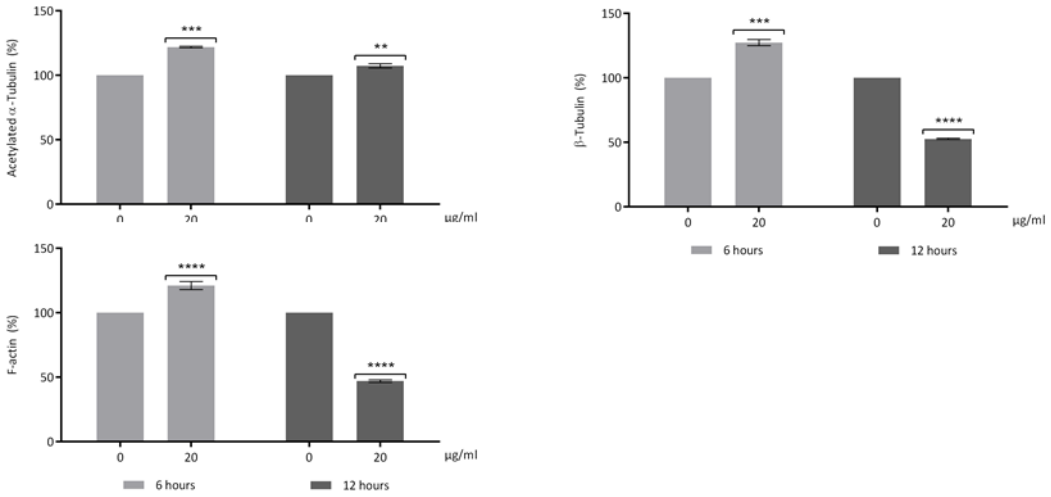

Figure 11: Influence of ZnO NPs in cytoskeleton structure of GC-1 spg cell line, a quantification analysis by immunocytochemistry. Immunocytochemistry images of acetylated α-tubulin (A), β-tubulin (B) and F-actin (A and B) and immunofluorescence quantification of α -tubulin, β-tubulin and F-actin protein levels (C) in GC-1 spg cell line. The cells were exposed to 0 and 20 µg/ml ZnO NPs for 6 hours and 12 hours. The protein levels are presented as a fold increase (%), which was plotted as mean ± SEM of three independent experiments and obtained by analysing at least 30 cells per condition from three independent experiments. ** P <0,01. *** p ≤0,001. **** p<0,0001. *for comparisons between concentrations and between time points, using two-way ANOVA.

Discussion

5. Discussion

The applications of ZnO NPs in Biomedicine are numerous, given their multiple advantages conferred by the physicochemical properties of these specific nanomaterials. However, ZnO NPs have significative cytotoxic effects on spermatogenesis. ZnO NPs have been reported as a dose and time dependent cytotoxic inducer in testis and in male germ cells. ROS production and DNA damage has been described as factors that induce apoptosis and cell cycle arrest in cells treated with ZnO NPs (Barkhordari et al., 2013; Han et al., 2016; Liu et al., 2016; Srivastav et al., 2017). These ZnO NPs cellular effects have negative repercussions on histological integrity of testis (Hussein et al., 2016; Mozaffari et al., 2015; Salman, 2017) and also in sperm quality as described (Abbasalipourkabir et al., 2015; Barkhordari et al., 2013; Han et al., 2016; Hussein et al., 2016; Srivastav et al., 2017; Talebi, Khorsandi and Moridian, 2013). Once, no study clarifies the consequences of ZnO NPs exposure in the first stage of spermatogenesis, in this study the cytotoxicity of this nanomaterial was tested in a spermatogonia cell line.

The results of the present work evidenced the cytotoxicity of ZnO NPs in GC-1 cells, dose and time dependent. Viability evaluation was assessed according the metabolic activity (Figure 8A) and the membrane integrity (Figure 8B) of GC-1 after their exposure to ZnO NPs. 6 hours with 10 μg/ml of ZnO NPs was enough to significantly decrease the metabolism of GC-1 cell, but not to damage its membrane integrity. Although, higher concentrations of ZnO NPs (20 μg/ml) besides reduce the metabolic activity of mouse spermatogonia cells, also induce the loss of cell membrane integrity. Furthermore, it is important to note that with the exception of cells exposed to 20 μg/ml of ZnO NPs, GC-1 viability does not significantly decrease after 12 hours of ZnO NPs exposure as expected. Which may indicate that ZnO NPs concentrations (<20 μg/ml) used were not sufficient to induce a permanent negative impact on cell, once GC-1 can recover from toxic effects of ZnO NPs (Figure 8).

These results are according with apoptosis and necrosis studies performed (Figure 8C). At 6 hours the number of apoptotic and/or necrotic cells was not significant. While the number of cells in late apoptosis and necrosis was significantly higher after 12 hours

of exposure to 20 µg/ml of ZnO, indicating that these cells are suffering a gradual permeabilization of cell membrane that culminates with membrane rupture leading to necrosis (Figure 8C). The significant loss of cell viability reported by trypan blue assay is in agreement with the cell death stage results from flow cytometry. Overall, ZnO NPs is a toxic nanomaterial to GC-1 cell line in a dose and time dependent manner, where only higher concentrations tested induce cell death with loss of cell metabolism and integrity.

The production of high levels of ROS induce serious alterations at spermatogonia cells by promoting biomolecular oxidation, that cause DNA fragmentation and consequently apoptosis or necrosis (Redza-Dutordoir and Averill-Bates, 2016; Sharma, Anderson and Dhawan, 2012). In the studies here described using GC-1 cells, ROS intracellular levels significantly increase after 6 hours of exposure to the maximum concentration evaluated here (20 µg/ml) and after 12 hours of exposure to 5, 10 and 20 µg/ml. Although, after 12 hours treatment with 20 µg/ml of ZnO NPs the increase was not higher than levels of cells exposed to lower concentrations, as might be expected (Figure 9). Is important to note that according with results from trypan blue exclusion methods, at 12 hours of incubation with 20 µg/ml of ZnO NPs, the cytoplasmatic membrane integrity was significantly diminished. Thus, the ROS detector is not correctly internalized by the cell and the intracellular ROS detection reaction does not occur properly, which could explain the unexpected lower ROS level at 12 hours of treatment with 20 µg/ml of ZnO NPs. Although, according to these results ZnO NPs exposure induce ROS production, and thus oxidative stress which may induce DNA damage in GC-1 cells in a dose and time dependent way (Figure 9).

Furthermore, it is important to mention that DNA damage and apoptosis can also occur by a consequence of high intracellular levels of Zn^{2+}. Besides in this study the Zn^{2+} release by ZnO NPs dissolution was not assessed, is indispensable report that others studies refer cell cytotoxicity as a consequence of Zn^{2+} homeostasis breakdown (Kao *et al.*, 2012). Several authors report Zn^{2+} increase as a product from ZnO NPs dissolution in lysosomes after cell uptake(García-Hevia *et al.*, 2016; Liu *et al.*, 2017; Nel *et al.*, 2009; Valdiglesias *et al.*, 2013).The intracellular zinc levels increase, exceeding the capacity of zinc homeostatic system. As a result, toxic zinc levels cause the mitochondrial membrane

potential breakdown, inducing mitochondrial generation of ROS, DNA fragmentation which activates caspases and leads to apoptosis. At even more elevated zinc concentration cell necrosis is the dominant form of cell death (Beyersmann, 2002; Kao *et al.*, 2012).

ZnO NPs have also influence in dynamics and structure of GC-1 cell line (Figure 12). The cytoskeleton is an interconnected network of intracellular filamentous composed of microtubules, intermediate filaments and actin filaments crucial for cell structural and shape maintenance, movement, division, and function (Fletcher and Mullins, 2010; Wickstead and Gull, 2011). Tubulin and actin are components of the cellular cytoskeleton, that assemble microtubules and actin filaments, respectively. Actin filaments were distributed in the cell membrane, while microtubules were located in the intracellular region between the cell nucleus and cell membrane (Fletcher and Mullins, 2010; Stricker, Falzone and Gardel, 2010). Microtubules and actin filaments are continuously undergoing polymerization depolymerization processes that are exquisitely controlled by intracellular proteins (Glozak *et al.*, 2005; Piperno, LeDizet and Chang, 1987). Acetylated α-tubulin have a role in stabilizing the structure of all microtubules, protecting microtubules from disruption (Liu *et al.*, 2019; Piperno, LeDizet and Chang, 1987), and also repairing the damage on microtubule (Janke and Montagnac, 2017)**.** Any interference with microtubule dynamics during cell division produces aberrant spindles leading to apoptosis, or to unbalanced chromosome distribution in the daughter cells (García-Hevia *et al.*, 2016). NPs disrupt the cytoskeleton architecture or cytoskeletal components in different types of cells, although this dysregulation is also dependent of cell type. Beyond shape modifications in cell morphology during evident cellular stress responses, the cytoskeleton disruption also causes alterations in cell signalling under sub-toxic conditions, including during exposure to NPs in which cell viability is unmodified or marginally decreased. Alterations on cytoskeleton components should be investigated as predictors not only of cell shape modifications but also of cell physiology in exposed cells to NPs (Ispanixtlahuatl-Meráz, Schins and Chirino, 2018).

In GC-1 cells is visible the increase of acetylated α-tubulin, a marker of microtubules stabilization, after higher exposure to ZnO NPs. The increase of acetylated

α-tubulin may occurs for protecting MT structure from damage induced by ZnO NPs as a recent study indicate (Liu *et al.*, 2019). Further, the dynamics of β-tubulin exposure also decreases after a long exposure to high concentration of ZnO NPs, which indicate that the microtubules are conditioned, the protein transport are compromised, altering the cellular dynamic (Figure 10B; Figure 11A and C). Besides that, β-actin (Figure 10C); does not significantly changed, but the F-actin (Figure 11) are reduced after 12 hours of exposure to ZnO NPs. Although, the immunocytochemistry analysis revealed an increase of β-tubulin and of F-actin after 6 hours of exposure (Figure 11). Tubulin and actin are two zinc-scavenging proteins that undergoes structural changes upon zinc binding (Eagle, Zombola and Himes, 1983; Strzelecka-Golaszewska, Prochniewicz and Drabikowski, 1978). According with a previous study, Zn^{2+} bind directly to tubulin, stimulating its assembly (Eagle, Zombola and Himes, 1983), and also induce F-actin polymerization and aggregation (Strzelecka-Golaszewska, Prochniewicz and Drabikowski, 1978), which is in concordance with the increase of β-tubulin and of F-actin fluorescence by immunocytochemistry analysis, respectively. At 12 hours, the decrease of F-actin and β-tubulin may be associated with increased ROS production (Choudhury *et al.*, 2017; Liu *et al.*, 2017).

Besides causing cytoskeleton alterations ZnO NPs were also reported as an inducer of nuclear enlargement and chromatin compaction (Choudhury *et al.*, 2017). According to immunocytochemistry images of DAPI-labeled nuclei, morphological changes in the nucleus are visible after exposure to ZnO NPs (Figure 11A and B). The nuclear envelope (NE) is a selective structural barrier composed of a pair of distinct membranes the inner (INM) and outer nuclear membranes (ONM) separated by the perinuclear space, that defined the barrier between the cytoplasm and nucleus (Crisp *et al.*, 2006). SUN and Klarsicht, ANC-1, Syne homology (KASH) proteins domains are type II integral membrane proteins embedded in the INM and ONM, respectively, which physically interact in the perinuclear space to form a physical connection of nucleoplasm and cytoskeleton, the LINC complex (Göb *et al.*, 2011; Haque *et al.*, 2006; Padmakumar *et al.*, 2005; Starr, 2011). LINC complexes are critical for nuclear integrity and play

fundamental roles in nuclear positioning, shaping and movement (Crisp *et al.*, 2006; Lu *et al.*, 2008).

The nucleoskeleton was also evaluated in GC-1 cells, Sun1 an inner nuclear envelope protein from LINC complex was decreased in presence of lower and higher concentrations of ZnO NPs. Sun1 is responsible for connection between chromosomes to the cytoplasmatic actin filaments, it is also important for completion of mammalian meiosis and its knockout in male mice halts spermatogenesis at prophase, leading to infertility (Chi *et al.*, 2009; Pereira *et al.*, 2019). Thus, Sun1 levels decrease (Figure 10D) in GC-1 cells could indicate that ZnO NPs may negatively condition spermatogenesis. Contrary to previous results where cell alterations were verified only at higher ZnO NPs concentrations, Sun1 intracellular levels decrease even in the presence of low ZnO NPs concentrations. This can be explained by its zinc finger domain (Haque *et al.*, 2006), which interact with DNA and mediate protein-protein interactions in response to zinc status (Bird *et al.*, 2003; O'Halloran, 1993). Zinc intracellular levels alterations can affect the interaction between Sun1 and DNA, which may compromise the mRNA export from the nucleus into the cytoplasm, affecting gene expression. Decreased intracellular Sun1 levels in the presence of ZnO NPs may be related to alterations in their expression (Li and Noegel, 2015; Wickramasinghe and Laskey, 2015).

Also, the nuclear envelope alterations may be an indirect consequence resulting from cytoskeleton disruption after exposure to NPs, leading to nuclear membrane disruption (Choudhury *et al.*, 2017). For a better understand of mechanism behind nuclear envelope alterations, it will be necessary verify ZnO NPs effects at KASH protein level in GC-1 cells, a nuclear protein that interact with cytoskeleton.

Metabolic cell activity reduction, cell membrane integrity loss, ROS production, DNA damage, cytoskeleton and nucleoskeleton alterations and cell death in the GC-1 cell line (Figure 12), are common consequences also reported by other studies that expose ZnO NPs to other cell types. However, the exact cytotoxic mechanism behind is not yet consensual. Some studies refer surface reactivity as the responsible for spontaneous ROS generation in cells exposed to ZnO NPs (Li *et al.*, 2016; Nel *et al.*, 2009; Sharma, Anderson and Dhawan, 2012), other studies refer Zn^{2+} release by the dissolution of ZnO NPs as the

cause of cytotoxicity (García-Hevia *et al.*, 2016; Liu *et al.*, 2017; Nel *et al.*, 2009; Valdiglesias *et al.*, 2013). Once this study does not evaluate the ZnO NPs dissolution or accumulation in GC-1 cells, these results are not capable to associate ROS production as the cause of cytotoxicity or as just a consequence of cytotoxicity induced by Zn^{2+} release.

Furthermore, is important to note that nanomaterials need to be evaluated also looking for its psychochemical properties because they conditionate its toxicokinetic, they determine the routes of exposure, and might lead to new biological interactions and unforeseen toxicities (Walker and Bucher, 2009). In addition, the relative risk of ZnO NPs in GC-1 cells cannot be assess only looking for concentration and time of exposure.

Conclusions and Future Perspectives

6. Conclusions and Futures Perspectives

ZnO NPs have significative cytotoxic effects on spermatogenesis, depending on dose and exposure time, indicating that a high concentration and a high time of exposure induce more toxicity. The toxicity is dependent of ROS production and inhibition of antioxidant activity, which induce DNA damage, cell cycle arrest, resulting in apoptosis of male germ cells, but also in Sertoli and Leydig cells which role of support and regulation of spermatogenesis are well known. Oxidative stress has also an important harmful effect on Sertoli cells, besides apoptosis, since the tight junctions suffer significative effects that compromise the support of all spermatogenesis. At histological level, sloughing and degeneration of male germ cells and also disorganization of germ cells layers as a consequence. Regarding Leydig cells, histological studies indicated a decrease of their number as a consequence of exposure to ZnO NPs. The serum levels of testosterone also decreased, which compromises the progression of spermatogenesis, that is testosterone dependent. These reductions were explained by the decrease of steroidogenic proteins expression in testes samples, the decrease of mitochondrial membrane potential and the increase of apoptosis in Leydig cells.

According with this work, at spermatogonia level (Figure 12):

1. ZnO NPs exposure induce cytotoxic effects in a dose and time dependent manner. However, low levels of ZnO NPs do not cause alterations in spermatogonia;
2. ROS production and DNA damage increased are a consequence of exposure to ZnO NPs in GC-1 cell;
3. Higher levels of ZnO NPs and bigger exposure periods induce apoptosis and necrosis as a consequence of ROS production and DNA damage increase;
4. Cytoskeletal alterations are a cytotoxic consequence of high levels of ZnO NPs exposure;
5. Low concentrations of ZnO NPs decrease Sun1 intracellular levels.

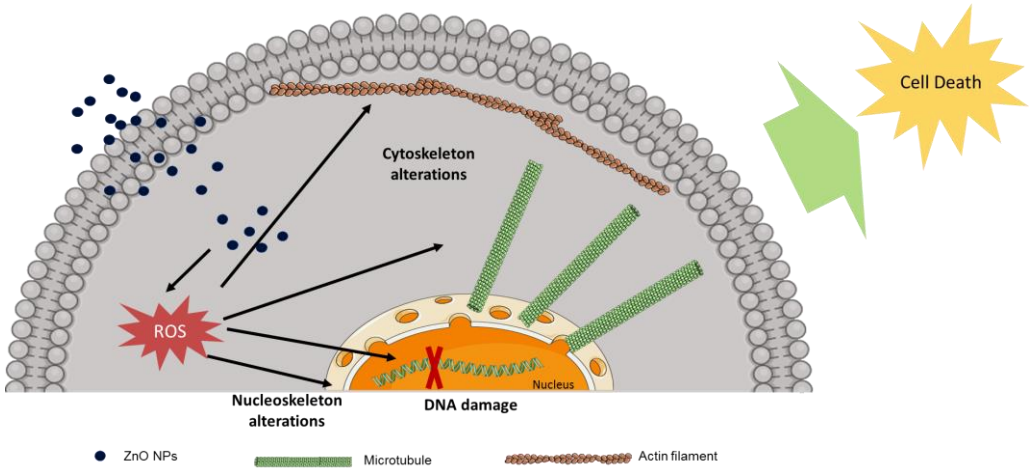

Figure 12: ZnO NPs cytotoxic effects in spermatogonia cell. ROS- Reactive Oxygen Species; DNA- Deoxyribonucleic Acid. (Adapted from: Liu *et al.*, 2017).

The study of ZnO NPs effects on male fertility is still poor, mainly at the in vitro level. The research is underway to better understand the mechanism of action of these nanomaterials behind cytoskeleton and nucleoskeleton alterations. Also, it will be interesting to extend the assays to the later stages of spermatogenesis. It is important understand if ZnO NPs is capable to compromise all the spermatogenesis or whether its harmful effects are reversible. Further, the sperm fertilization capacity is an important parameter that should be determined in mammalian exposed to ZnO NPs, in order to understand their direct effect in male fertility. In future, is important address cytotoxicity and histotoxicity studies in human samples, given the scarcity of such approach.

Besides that, it will be interesting to investigate ways to control the toxic effects of ZnO NPs reported so far. Several studies have developed new forms of ZnO NPs encapsulation with other materials that diminished its natural cytotoxicity, thus the toxicity of these new nanocomplexes also needs to be investigated in testicular cells. In addition, it is important to note that all studies evaluate ZnO NPs toxicity based on concentration and exposure time, but the effects of any NP also depend on their physicochemical properties. Thus, future studies should be conducted to assess their effects on male reproductive system based on size, surface area and method of synthesis.

References

References

1. ABASPOUR APORVARI, H. *et al.* - The effect of oral administration of zinc oxide nanoparticles on quantitative and qualitative properties of arabic ram sperm and some antioxidant parameters of seminal plasma in the non-breeding season. **Archives of Razi Institute**. 73:2 (2018) 121–129.

2. ABBASALIPOURKABIR, Roghayeh *et al.* - Toxicity of zinc oxide nanoparticles on adult male Wistar rats. **Food and Chemical Toxicology**. 84: (2015) 154–160.

3. AFIFI, Mohamed; ALMAGHRABI, Omar A.; KADASA, Naif Mohammed - Ameliorative Effect of Zinc Oxide Nanoparticles on Antioxidants and Sperm Characteristics in Streptozotocin-Induced Diabetic Rat Testes. **BioMed Research International**. 2015:1 (2015) 1–6.

4. ALKALADI, Ali; ABDELAZIM, Aaser Mohamed; AFIFI, Mohamed - Antidiabetic activity of zinc oxide and silver nanoparticles on streptozotocin-induced diabetic rats. **International Journal of Molecular Sciences**. 15:2 (2014) 2015–2023.

5. APPIEROT, Guy *et al.* - Enhanced antibacterial actiwity of nanocrystalline ZnO due to increased ROS-mediated cell injury. **Advanced Functional Materials**. 19:6 (2009) 842–852.

6. BARKHORDARI, Abolfazl *et al.* - Effect of zinc oxide nanoparticles on viability of human spermatozoa. **Iranian journal of reproductive medicine**. 11:9 (2013) 767–771.

7. BERARDIS, Barbara DE *et al.* - Exposure to ZnO nanoparticles induces oxidative stress and cytotoxicity in human colon carcinoma cells. **Toxicology and Applied Pharmacology**. 246:3 (2010) 116–127.

8. BEYERSMANN, Detmar - Homeostasis and cellular functions of zinc. **Materials Science and Engineering Technology**. 33:12 (2002) 764–769.

9. BIRD, Amanda J. *et al.* - Zinc fingers can act as Zn2+ sensors to regulate transcriptional activation domain function. **EMBO Journal**. 22:19 (2003) 5137–

5146.

10. BROWN, Robert B.; AUDET, Julie - Current techniques for single-cell lysis. **Journal of the Royal Society Interface**. 5: (2008) S131–S138.

11. BUZEA, Cristina; PACHECO, Ivan I.; ROBBIE, Kevin - Nanomaterials and nanoparticles: sources and toxicity. **Biointerphases**. 2:4 (2007) 17–71.

12. CHEN, Aijie *et al.* - Evaluation of the effect of time on the distribution of zinc oxide nanoparticles in tissues of rats and mice: A systematic review. **IET Nanobiotechnology**. 10:3 (2016) 97–106.

13. CHENG, C.Yan *et al.* - Regulation of Spermatogenesis in the Microenvironment of the Seminiferous Epithelium: New Insights and Advances. **Molecular and Cellular Endocrinology**. 315:1–2 (2010) 49–56.

14. CHI, Ya Hui *et al.* - Requirement for Sun1 in the expression of meiotic reproductive genes and piRNA. **Development**. 136:6 (2009) 965–973.

15. CHOUDHURY, Samrat Roy *et al.* - Zinc oxide nanoparticles-induced reactive oxygen species promotes multimodal cyto- and epigenetic toxicity. **Toxicological Sciences**. 156:1 (2017) 261–274.

16. CRISP, Melissa *et al.* - Coupling of the nucleus and cytoplasm: Role of the LINC complex. **Journal of Cell Biology**. 172:1 (2006) 41–53.

17. DARZYNKIEWICZ, Z. *et al.* - Features of apoptotic cells measured by flow cytometry. **Cytometry**. 13:8 (1992) 795–808.

18. DEMCHENKO, Alexander P. - Beyond annexin V: Fluorescence response of cellular membranes to apoptosis. **Cytotechnology**. 65:2 (2013) 157–172.

19. DOWLING, A. *et al.* - Nanoscience and nanotechnologies: opportunities and uncertainties. **Neuroradiology**. 46:7 (2004) 618–618.

20. DUTTA, R. K. *et al.* - Studies on antibacterial activity of ZnO nanoparticles by ROS induced lipid peroxidation. **Colloids and Surfaces B: Biointerfaces**. 94:2012) 143–

150.

21. EAGLE, Geoffrey R.; ZOMBOLA, Randall R.; HIMES, Richard H. - Tubulin-Zinc Interactions: Binding and Polymerization Studies. **Biochemistry**. 22:1 (1983) 221–228.

22. EIXENBERGER, Josh E. *et al.* - Defect Engineering of ZnO Nanoparticles for Bioimaging Applications. **ACS Applied Materials & Interfaces**. 11:28 (2019) 24933–24944.

23. EL-GHARBAWY, Rehab Mohmed; EMARA, Ashraf Mahmoud; ABU-RISHA, Sally El Sayed - Zinc oxide nanoparticles and a standard antidiabetic drug restore the function and structure of beta cells in Type-2 diabetes. **Biomedicine and Pharmacotherapy**. 84: (2016) 810–820.

24. EWING, L. L.; ZIRKIN, B. - Leydig cell structure and steroidogenic function. **Recent Progress in Hormone Research**. 39: (1983) 599–635.

25. FLETCHER, Daniel A; MULLINS, R.Dyche - Cell mechanisms and cytoskeleton. **Nature**. 463:7280 (2010) 485–492.

26. GARCÍA-HEVIA, Lorena *et al.* - Nano-ZnO leads to tubulin macrotube assembly and actin bundling, triggering cytoskeletal catastrophe and cell necrosis. **Nanoscale**. 8:21 (2016) 10963–10973.

27. GLOZAK, Michele A. *et al.* - Acetylation and deacetylation of non-histone proteins. **Gene**. 363: (2005) 15–23.

28. GÖB, Eva *et al.* - Expression of individual mammalian Sun1 isoforms depends on the cell type. **Communicative & Integrative Biology**. 4:4 (2011) 440–442.

29. GOMES, Ana; FERNANDES, Eduarda; LIMA, José L. F. C. - Fluorescence probes used for detection of reactive oxygen species. **Journal of Biochemical and Biophysical Methods**. 65:2–3 (2005) 45–80.

30. GRIFFITHS, Gareth - **Fine Structure Immunocytochemistry**

31. GRISWOLD, Michael D. - Spermatogenesis: The commitment to Meiosis. **Physiological Reviews**. 96:1 (2016) 1–17.

32. GU, Baoxiang *et al.* - ZnO quantum dot labeled immunosensor for carbohydrate antigen 19-9. **Biosensors and Bioelectronics**. 26:5 (2011) 2720–2723.

33. HALLIWELL, Barry; WHITEMAN, Matthew - Measuring reactive species and oxidative damage in vivo and in cell culture: How should you do it and what do the results mean? **British Journal of Pharmacology**. 142:2 (2004) 231–255.

34. HAN, Zhe *et al.* - Cytotoxic effects of ZnO nanoparticles on mouse testicular cells. **International Journal of Nanomedicine**. 11: (2016) 5187–5203.

35. HANLEY, Cory *et al.* - Preferential killing of cancer cells and activated human T cells using ZnO nanoparticles. **Nanotechnology**. 19:29 (2008) 1–20.

36. HAO, Yanan *et al.* - Molecular evidence of offspring liver dysfunction after maternal exposure to zinc oxide nanoparticles. **Toxicology and Applied Pharmacology**. 329: (2017) 318–325.

37. HAQUE, F. *et al.* - SUN1 Interacts with Nuclear Lamin A and Cytoplasmic Nesprins To Provide a Physical Connection between the Nuclear Lamina and the Cytoskeleton. **Molecular and Cellular Biology**. 26:10 (2006) 3738–3751.

38. HE, Lili *et al.* - Antifungal activity of zinc oxide nanoparticles against Botrytis cinerea and Penicillium expansum. **Microbiological Research**. 166:3 (2011) 207–215.

39. HEILIGTAG, Florian J.; NIEDERBERGER, Markus - The fascinating world of nanoparticle research. **Materials Today**. 16:7/8 (2013) 262–271.

40. HEINLAAN, Margit *et al.* - Toxicity of nanosized and bulk ZnO, CuO and TiO2 to bacteria Vibrio fischeri and crustaceans Daphnia magna and Thamnocephalus platyurus. **Chemosphere**. 71:7 (2008) 1308–1316.

41. HELLANI, Ali *et al.* - Developmental and hormonal regulation of the expression of oligodendrocyte-specific protein/claudin 11 in mouse testis. **Endocrinology**. 141:8

(2000) 3012–3019.

42. HOLSTEIN, Adolf Friedrich; SCHULZE, Wolfgang; DAVIDOFF, Michail - Understanding spermatogenesis is a prerequisite for treatment. **Reproductive Biology and Endocrinology**. 1: (2003) 1–16.

43. HUANG, Zhongbing *et al.* - Toxicological effect of ZnO nanoparticles based on bacteria. **Langmuir**. 24:8 (2008) 4140–4144.

44. HULLA, J. E.; SAHU, S. C.; HAYES, A. W. - Nanotechnology: History and future. **Human and Experimental Toxicology**. 34:12 (2015) 1318–1321.

45. HUSSEIN, Mohamed M. A. *et al.* - Querectin Alleviates Zinc Oxide Nanoreprotoxicity in Male Albino Rats. **J Biochem Molecular Toxicology**. 30:10 (2016) 489–496.

46. ISPANIXTLAHUATL-MERÁZ, Octavio; SCHINS, Roel P. F.; CHIRINO, Yolanda I. - Cell type specific cytoskeleton disruption induced by engineered nanoparticles. **Environmental Science: Nano**. 5:2 (2018) 228–245.

47. JALAL, Razieh *et al.* - ZnO nanofluids: Green synthesis, characterization, and antibacterial activity. **Materials Chemistry and Physics**. 121:1–2 (2010) 198–201.

48. JANKE, Carsten; MONTAGNAC, Guillaume - Causes and Consequences of Microtubule Acetylation. **Current Biology**. 27:23 (2017) 1287–1292.

49. JEEVANANDAM, Jaison *et al.* - Review on nanoparticles and nanostructured materials: History, sources, toxicity and regulations. **Beilstein Journal of Nanotechnology**. 9:1 (2018) 1050–1074.

50. JIANG, Jinhuan; PI, Jiang; CAI, Jiye - The Advancing of Zinc Oxide Nanoparticles for Biomedical Applications. **Bioinorganic Chemistry and Applications**. 2018:3 (2018) 1–18.

51. JONES, Nicole *et al.* - Antibacterial activity of ZnO nanoparticle suspensions on a broad spectrum of microorganisms. **FEMS Microbiol Lett**. 279: (2008) 71–76.

52. KANG, Yanjun *et al.* - Multicolor bioimaging with biosynthetic zinc nanoparticles and their application in tumor detection. **Scientific Reports**. 7:October 2016 (2017) 1–11.

53. KAO, Yi Yun *et al.* - Zinc oxide nanoparticles interfere with zinc ion homeostasis to cause cytotoxicity. **Toxicological Sciences**. 125:2 (2012) 462–472.

54. KHOOBBAKHT, Zeinab *et al.* - Comparative effects of zinc oxide, zinc oxide nanoparticle and zinc-methionine on hatchability and reproductive variables in male Japanese quail. **Animal Reproduction Science**. 192: (2018) 84–90.

55. KOLODZIEJCZAK-RADZIMSKA, Agnieszka; JESIONOWSKI, Teofil - Zinc oxide-from synthesis to application: A review. **Materials**. 7:4 (2014) 2833–2881.

56. KRETSER, D. M. De *et al.* - Spermatogenesis. **Human Reproduction**. 13: (1998) 1–8.

57. KRÓL, A. *et al.* - Zinc oxide nanoparticles: Synthesis, antiseptic activity and toxicity mechanism. **Advances in Colloid and Interface Science**. 249: (2017) 37–52.

58. KUANG, Huijuan *et al.* - Size dependent effect of ZnO nanoparticles on endoplasmic reticulum stress signaling pathway in murine liver. **Journal of Hazardous Materials**. 317: (2016) 119–126.

59. LAN, Zhou; YANG, Wan Xi - Nanoparticles and spermatogenesis: How do nanoparticles affect spermatogenesis and penetrate the blood-testis barrier. **Nanomedicine**. 7:4 (2012) 579–596.

60. LI, Lijia *et al.* - Zinc oxide nanoparticles-induced epigenetic change and G2/M arrest are associated with apoptosis in human epidermal keratinocytes. **International Journal of Nanomedicine**. 11: (2016) 3859–3874.

61. LI, Mei; ZHU, Lizhong; LIN, Daohui - Toxicity of ZnO nanoparticles to escherichia Coli: Mechanism and the influence of medium components. **Environmental Science and Technology**. 45:5 (2011) 1977–1983.

62. LI, Michelle W. M. *et al.* - Tumor necrosis factor α reversibly disrupts the blood-testis barrier and impairs Sertoli-germ cell adhesion in the seminiferous

epithelium of adult rat testes. **Journal of Endocrinology**. 190:2 (2006) 313–329.

63. LIN, Yuh-Feng *et al.* - The role of hypoxia-inducible factor-1α in zinc oxide nanoparticle-induced nephrotoxicity in vitro and in vivo. **Particle and Fibre Toxicology**. 13:1 (2015) 1–14.

64. LI, Ping; NOEGEL, Angelika A. - Inner nuclear envelope protein SUN1 plays a prominent role in mammalian mRNA export. Nucleic Acids Research. 43:20 (2015) 9874–9888.

65. LIPOVSKY, Anat *et al.* - Antifungal activity of ZnO nanoparticles-the role of ROS mediated cell injury. **Nanotechnology**. 22:10 (2011) 1–5.

66. LIU, Jia *et al.* - Zinc oxide nanoparticles induce toxic responses in human neuroblastoma SHSY5Y cells in a size-dependent manner. **International Journal of Nanomedicine**. 12: (2017) 8085–8099.

67. LIU, Jia *et al.* - Key Role of Microtubule and Its Acetylation in a Zinc Oxide Nanoparticle–Mediated Lysosome–Autophagy System. **Small**. 15:25 (2019) 1901073.

68. LIU, Qian *et al.* - Sublethal effects of zinc oxide nanoparticles on male reproductive cells. **Toxicology in Vitro**. 35: (2016) 131–138.

69. LIU, Yanlan *et al.* - Fluorescence-enhanced gadolinium-doped zinc oxide quantum dots for magnetic resonance and fluorescence imaging. **Biomaterials**. 32:4 (2011) 1185–1192.

70. LU, Haijiao *et al.* - An overview of nanomaterials for water technology. **Advances in Materials Science and Engineering**. 2016: (2017) 1–10.

71. LU, Wenshu *et al.* - Sun1 forms immobile macromolecular assemblies at the nuclear envelope. **Biochimica et Biophysica Acta (BBA) - Molecular Cell Research**. 1783:12 (2008) 2415–2426.

72. MADHUMITHA, Gunabalan; ELANGO, Ganesh; ROOPAN, Selvaraj Mohana - Biotechnological aspects of ZnO nanoparticles: overview on synthesis and its

applications. **Applied Microbiology and Biotechnology**. 100:2 (2016) 571–581.

73. MIKRAJUDDIN *et al.* - Luminescent polymer electrolytes prepared by growing ZnO nanoparticles in the matrix of polyethylene glycol. **Journal of the Electrochemical Society**. 149:5 (2002).

74. MISHRA, Pawan K. *et al.* - Zinc oxide nanoparticles: a promising nanomaterial for biomedical applications. **Drug Discovery Today**. 22:12 (2017) 1825–1834.

75. MOZAFFARI, Ziba *et al.* - Histopathological evaluation of the toxic effects of zinc oxide (ZnO) nanoparticles on testicular tissue of NMRI adult mice. **Advanced Studies in Biology**. 7:6 (2015) 275–291.

76. NAGAJYOTHI, P. C. *et al.* - Characterization, antibacterial, antioxidant, and cytotoxic activities of ZnO nanoparticles using Coptidis Rhizoma. **Bioorganic and Medicinal Chemistry Letters**. 24:17 (2014) 4298–4303.

77. NEL, Andre E. *et al.* - Understanding biophysicochemical interactions at the nano-bio interface. **Nature Materials**. 8:7 (2009) 543–557.

78. NOVUS BIOLOGICALS - Immunocytochemistry (ICC) Handbook.

79. O'DONNELL, Brittany *et al.* - ZnO nanoparticles enhanced germ cell apoptosis in Caenorhabditis elegans , in comparison with ZnCl 2. **Toxicological Sciences**. 156:2 (2017) 336–343.

80. O'HALLORAN, Thomas V. - Transition metals in control of gene expression. **Science**. 261:5122 (1993) 715–725.

81. OSTROVSKY, Stella *et al.* - Selective cytotoxic effect of ZnO nanoparticles on glioma cells. **Nano Research**. 2:11 (2009) 882–890.

82. PADMAKUMAR, V. C. *et al.* - The inner nuclear membrane protein Sun1 mediates the anchorage of Nesprin-2 to the nuclear envelope. **Journal of Cell Science**. 118:15 (2005) 3419–3430.

83. PASQUET, Julia *et al.* - Antimicrobial activity of zinc oxide particles on five micro-

organisms of the Challenge Tests related to their physicochemical properties. **International Journal of Pharmaceutics**. 460:1–2 (2014) 92–100.

84. PAVELESCU, L. A. - On reactive oxygen species measurement in living systems. **Journal of medicine and life**. 8:Special Issue (2015) 38–42.

85. PAYNE, Anita H.; HARDY, Matthew P. - The Leydig Cell in Health and Disease. (Contemporary Endocrinology) 2007 Edition, Kindle Edition

86. PEACH, Mandy *et al.* - Solubilization of Proteins: The Importance of Lysis Buffer Choice. **Western Blotting: Methods and Protocols (2015)** p. 49–60.

87. PEREIRA, Cátia D. *et al.* - Nuclear envelope dynamics during mammalian spermatogenesis: new insights on male fertility. **Biological Reviews**. 94:4 (2019) 1195–1219.

88. PINA, S. *et al.* - In Vitro performance assessment of new brushite-forming Zn- and ZnSr-substituted b -TCP bone cements. **Journal of Biomedical Materials Research Part B: Applied Biomaterials**. Hoboken. 94:2 (2010) 414–420.

89. PIPERNO, Gianni; LEDIZET, Michel; CHANG, Xiao-jia - Microtubules Containing Acetylated a-Tubulin in Mammalian Cells in Culture. **The Journal of Cell Biology**. 104: (1987) 289–302.

90. POSSEL, Heiko *et al.* - 2,7-Dihydrodichlorofluorescein diacetate as a fluorescent marker for peroxynitrite formation. **FEBS Letters**. 416:2 (1997) 175–178.

91. PRASAD, T. N. V. K. V. *et al.* - Effect of nanoscale zinc oxide particles on the germination, growth and yield of peanut. **Journal of Plant Nutrition**. 35:6 (2012) 905–927.

92. RAD, Samira Shahriyari; SANI, Ali Mohamadi; MOHSENI, Sharareh - Biosynthesis, characterization and antimicrobial activities of zinc oxide nanoparticles from leaf extract of Mentha pulegium (L.). **Microbial Pathogenesis**. 131: (2019) 239–245.

93. RAMPERSAD, Sephra N. - Multiple Applications of Alamar Blue as an Indicator of Metabolic Function and Cellular Health in Cell Viability Bioassays. **Sensors**. Basel.

12:9 (2012) 12347–12360.

94. RASMUSSEN, John W. *et al.* - Zinc oxide nanoparticles for selective destruction of tumor cells and potential for drug delivery applications. **Expert Opinion on Drug Delivery**. 7:9 (2010) 1063–1077.

95. REDZA-DUTORDOIR, Maureen; AVERILL-BATES, Diana A. - Activation of apoptosis signalling pathways by reactive oxygen species. **Biochimica et Biophysica Acta**. 1863:12 (2016) 2977–2992.

96. REUTELINGSPERGER, C. P. M.; HEERDE, W. L. VAN - Annexin V, the regulator of phosphatidylserine-catalyzed inflammation and coagulation during apoptosis. **Cellular and Molecular Life Sciences**. 53:6 (1997) 527–532.

97. RODRÍGUEZ, Juan *et al.* - Synthesis and characterization of ZnO nanorod films for photocatalytic disinfection of contaminated water. **Thin Solid Films**. 519:2 (2010) 729–735.

98. SABIR, Sidra; ARSHAD, Muhammad; CHAUDHARI, Sunbal Khalil - Zinc oxide nanoparticles for revolutionizing agriculture: Synthesis and applications. **Scientific World Journal**. 2014: (2014) 1–8.

99. SALMAN, Ruqayah Ali - The Influence of ZnO NPs on Reproductive System Tissues of Albino Male Mice. Histopathological Study. **International Journal of Science and Research**. 6:7 (2017) 2021–2025.

100. SAWAI, J.; YOSHIKAWA, T. - Quantitative evaluation of antifungal activity of metallic oxide powders (MgO, CaO and ZnO) by an indirect conductimetric assay. **Journal of Applied Microbiology**. 96:4 (2004) 803–809.

101. SETYAWATI, Magdiel I.; TAY, Chor Yong; LEONG, David T. - Effect of zinc oxide nanomaterials-induced oxidative stress on the p53 pathway. **Biomaterials**. 34:38 (2013) 10133–10142.

102. SHARMA, Harshita *et al.* - Development and characterization of metal oxide nanoparticles for the delivery of anticancer drug. **Artificial Cells,**

Nanomedicine and Biotechnology. 44:2 (2016) 672–679.

103. SHARMA, Rakesh; AGARWA, Ashok - Spermatogenesis: An Overview. In **Sperm Chromatin**. p. 19–44.

104. SHARMA, Vyom; ANDERSON, Diana; DHAWAN, Alok - Zinc oxide nanoparticles induce oxidative DNA damage and ROS-triggered mitochondria mediated apoptosis in human liver cells (HepG2). **Apoptosis**. 17:8 (2012) 852–870.

105. SINGH, Kulvinder *et al.* - Synthesis of highly luminescent water stable ZnO quantum dots as photoluminescent sensor for picric acid. **Journal of Luminescence**. 154: (2014) 148–154.

106. SMITH, P. K. *et al.* - Measurement of protein using bicinchoninic acid. **Analytical Biochemistry**. 150:1 (1985) 76–85.

107. SOLIER, Stéphanie; POMMIE, Yves - The Nuclear γ-H2AX Apoptotic Ring: Implications for Cancers and Autoimmune Diseases. **Cellular and Molecular Life Sciences Molecular Life Science**. 71:12 (2014) 2289–2297.

108. SOUZA, Roberta C. *et al.* - Antibacterial activity of zinc oxide nanoparticles synthesized by solochemical process. **Brazilian Journal of Chemical Engineering**. 36:2 (2019) 885–893.

109. SRIVASTAV, Anurag Kumar *et al.* - Genotoxicity evaluation of zinc oxide nanoparticles in Swiss mice after oral administration using chromosomal aberration, micronuclei, semen analysis, and RAPD profile. **Toxicology and Industrial Health**. 33:11 (2017) 821–834.

110. STARR, Daniel - KASH and SUN proteins. **Current Biology**. 21:11 (2011) 414–415.

111. STOIMENOV, Peter K. *et al.* - Metal oxide nanoparticles as bactericidal agents. **Langmuir**. 18:17 (2002) 6679–6686.

112. STRICKER, Jonathan; FALZONE, Tobias; GARDEL, Margaret - Mechanics of the F-actin Cytoskeleton. **Journal of biomechanism**. 43:1 (2010) 1–7.

113. STROBER, Warren - **Trypan Blue Exclusion Test of Cell Viability**

114. STRZELECKA-GOLASZEWSKA, H.; PROCHNIEWICZ, E.; DRABIKOWSKI, W. - Interaction of actin with divalent cations. **European Journal of Biochemistry**. 227: (1978) 219–227.

115. TALEBI, Ali Reza; KHORSANDI, Layasadat; MORIDIAN, Mahnaz - The effect of zinc oxide nanoparticles on mouse spermatogenesis. **Journal of Assisted Reproduction and Genetics**. 30:9 (2013) 1203–1209.

116. TRIPATHY, Nirmalya *et al.* - Enhanced anticancer potency using an acid-responsive ZnO-incorporated liposomal drug-delivery system. **Nanoscale**. 7:9 (2015) 4088–4096.

117. UMRANI, Rinku D.; PAKNIKAR, Kishore M. - Zinc oxide nanoparticles show antidiabetic activity in streptozotocin- induced Type 1 and 2 diabetic rats. **Nanomedicine**. 9:1 (2014) 89–104.

118. UZARSKI, Joseph S. *et al.* - Essential Design Considerations for the Resazurin Reduction Assay to Noninvasively Quantify Cell Expansion within Perfused Extracellular Matrix Scaffolds. **Biomaterials**. Amsterdam. 129: (2017) 163–175.

119. VALDIGLESIAS, Vanessa *et al.* - Neuronal cytotoxicity and genotoxicity induced by zinc oxide nanoparticles. **Environment International**. 55: (2013) 92–100.

120. VERMES, István *et al.* - A novel assay for apoptosis Flow cytometric detection of phosphatidylserine expression on early apoptotic cells using fluorescein labelled Annexin V. **Journal of Immunological Methods**. 184:1 (1995) 39–51.

121. WAHBA, Nashwa S. *et al.* - Efficacy of zinc oxide nanoparticles in attenuating pancreatic damage in a rat model of streptozotocin-induced diabetes. **Ultrastructural Pathology**. 40:6 (2016) 358–373.

122. WALKER, Nigel J.; BUCHER, John R. - A 21st century paradigm for evaluating the health hazards of nanoscale materials? **Toxicological Sciences**. 110:2 (2009) 251–254.

123. WANG, Caixia *et al.* - ZnO Nanoparticles Treatment Induces Apoptosis by Increasing Intracellular ROS Levels in LTEP-a-2 Cells. **BioMed Research International**. 2015 (2015) 1–9.

124. WANG, Jiao *et al.* - Exploration of Zinc Oxide Nanoparticles as a Multitarget and Multifunctional Anticancer Nanomedicine. **ACS Applied Materials and Interfaces**. 9:46 (2017) 39971–39984.

125. WICKRAMASINGHE, Vihandha O.; LASKEY, Ronald A. - Control of mammalian gene expression by selective mRNA export. Nature Reviews Molecular Cell Biology. 16:7 (2015) 431–442.

126. WICKSTEAD, Bill; GULL, Keith - The evolution of the cytoskeleton. **Journal of Cell Biology**. 194:4 (2011) 513–525.

127. XIONG, Huan-ming - ZnO Nanoparticles Applied to Bioimaging and Drug Delivery. **Advanced Materials**. 25:37 (2013) 5329–5335.

128. XIONG, Huan Ming *et al.* - Stable aqueous ZnO@polymer core-shell nanoparticles with tunable photoluminescence and their application in cell imaging. **Journal of the American Chemical Society**. 130:24 (2008) 7522–7523.

129. YOSHIKAWA, Ariane Harumi; POSSEBON, Lucas; COSTA, Sara De Souza - Adverse effects of Metal-based Nanoparticles on Male Reproductive Cells. In **Top 10 Contributions on Environmental Health**. p. Chapter 8.

130. ZHANG, Lingling *et al.* - Investigation into the antibacterial behaviour of suspensions of ZnO nanoparticles (ZnO nanofluids). **Journal of Nanoparticle Research**. 9:3 (2007) 479–489.

131. ZHANG, Zheng Yong; XIONG, Huan Ming - Photoluminescent ZnO nanoparticles and their biological applications. **Materials**. 8:6 (2015) 3101–3127.

132. ZHAO, Di *et al.* - Luminescent ZnO quantum dots for sensitive and selective detection of dopamine. **Talanta**. 107: (2013) 133–139.

Appendix 1

Appendix 1

- **Culture cell solutions**
  - **Complete DMEM medium**

For a final volume of 500 ml, dilute 55 ml of 10% FBS and 5 ml of Pen-Strep. Sterilize by filtering through a 0,2 µm filter and store at 4ºC.

  - **1x PBS**

For a final volume of 500 ml, dissolve one pack of BupH Modified Dulbecco's Phosphate Buffered Saline Pack (Pierce) in deionized H2O.

Sterilize by filtering through a 0,2 µm filter and store at 4°C.

- **Flow Cytometry Solutions**
  - **Binding buffer (10 g/L)**

For a final volume of 50 ml dissolve 0,5 g of Ca^{2+} in 1x PBS.

  - **H_20_2 treatment (100 mM)**

In 10 ml of 1x PBS, 56,8 µl of 50% H_20_2 (d=1,2) was diluted.

- **Immunoblotting Solutions:**
  - **10% APS**

In 1 ml of deionized H2O dissolve 0,1 g of APS.

  - **10% SDS**

In 10 ml of deionized H2O dissolve 1 g of SDS.

  - **1 M Tris (pH 6,8) solution**

To 150 ml of deionized H2O add: 30,3 g Tris base

Adjust the pH to 6,8 and adjust the final volume to 250 ml with deionized H_2O.

- **Loading gel buffer (4x)**

	V=10 ml (pH 6,8)
Tris 1M (ml)	2,5
SDS (g)	0,8
Glicerol (ml)	4
β-Mercaptoetanol (ml)	2
Azul bromofenol (mg)	1

Adjust the volume to 10 ml with deionized H2O. Store in the dark at room temperature.

- **LGB (lower gel buffer) (4x)**

To 900 ml of deionized H_2O add: 181,65 g of Tris and 4 g of SDS

Mix until the solutes have dissolved. Adjust pH to 8,9 and the volume to 1 L with deionized H_2O.

- **UGB (Upper gel buffer) (4x)**

To 900 ml of deionized H_2O add: 75,69 g of Tris

Mix until the solute has dissolved. Adjust the pH to 6.8 and the volume to 1 L with deionized H_2O.

- **Resolving (lower) gel solution**

1 system – 1,5 mm	**5%**	**20%**
ddH_2O (ml)	18,59	7,34
Acrylamide/bis-Acrylamide (29:1) (ml)	3,75	15
LGB (ml)	7,5	7,5
APS (µL)	150	150
TEMED (µL)	15	15

- **Stacking (upper) gel solution**

1 system – 1,5 mm	**3,5%**
ddH_2O (ml)	13,83
Acrylamide/bis-Acrylamide (29:1) (ml)	1,75
UGB (ml)	4
SDS	200
APS (µL)	200
TEMED (µL)	20

- **10x Running buffer**

	V= 1 L (pH 8,3)
Tris (g)	30,3
Glycine (g)	144,2
SDS (g)	10

Dissolve in deionized H_2O.

- **10x Transfer buffer**

	V= 1 L (pH 8,3)
Tris (g)	30,3
Glycine (g)	144,1

For 1x transfer buffer: adjust the volume to 800 ml with deionized H_2O and add 200 ml of methanol.

- **10x TBS**

	V= 1 L (pH 8)
Tris (g)	12,11
NaCl (g)	87,66

- **10x TBS-T**

	V= 1 L (pH 8)
Tris (g)	12.11
NaCl (g)	87,66
Tween-20 (ml)	10

- **Stripping Mild Solution**

	V= 500 ml (pH 2,2)
Glycine (g)	7,5
SDS (g)	0,5
Tween-20 (ml)	5

Dissolve in deionized H_2O. Store at 4ºC in the dark.

- **Immunocytochemistry Solutions**
  - **3,7% PFA**

For a final volume of 50 ml, dilute 5 ml of PFA (37%) in 1x PBS. Store at 4ºC in the dark.

  - **0,2% Triton X-100 solution**

For a final volume of 50 ml, dilute 100 µl of Triton X-100 solution in 1x PBS. Store at 4ºC.

  - **Blocking Solution (3%BSA)**

For a final volume of 50 ml, dissolve 1,5 g of BSA in 1x PBS. Store at 4ºC.